RATE EFFECT IN A CYLINDER SUBJECTED TO IMPACT

By

LIRAN HADAD

A THESIS PRESENTED TO THE GRADUATE SCHOOL
OF THE UNIVERSITY OF FLORIDA IN PARTIAL FULFILLMENT
OF THE REQUIREMENTS FOR THE DEGREE OF
MASTER OF SCIENCE

UNIVERSITY OF FLORIDA

2011

In loving memory of my Mom, who even though she was sick, encouraged me to complete my degree

ACKNOWLEDGMENTS

I would like to express my heartfelt gratitude to my thesis advisor, Professor Theodor Krauthammer for his time, guidance and advice throughout the whole period of time. I would also like to thank my thesis committee member, Dr Serdar Astarlioglu for his time and assistance. Next, I would like to thank Dr Long Hoang Bui for his advice and teaching on the finite element software. I would also like to thank my friend and research partner, Mr. Avshalom Ganz for the effort putting in this research. Furthermore I am honored and grateful for Ministry of Defense, Israel, on the research founding and for University of Florida on the scholarship granted to me. I am grateful to Dr Doron Havazelet , Professor Oren Vilnay, and Professor David ornai from Ben-Gurion University, Israel, who offer me the opportunity to study aboard. In addition, I thank all my fellow colleagues at the Center for Infrastructure Protection and Physical Security (CIPPS), the Chabad family, and my friends in Gainesville for their love and support which made my stay in USA a wonderful experience. I owe my loving thanks to my family back in Israel. They have lost a lot due to my research abroad. Without their encouragement and understanding it would have been impossible for me to finish this work. Lastly, I would like to express my gratitude to my wife who made a huge sacrifice and accompany me here for study, and to my precious son and to my new beautiful daughters for sharing their daddy time with my research.

TABLE OF CONTENTS

page

LIST OF TABLES

LIST OF FIGURES

Figure page

Abstract of Thesis Presented to the Graduate School
of the University of Florida in Partial Fulfillment of the
Requirements for the Degree of Master of Science

RATE EFFECT IN A CYLINDER SUBJECTED TO IMPACT

By

Liran Hadad

August 2011

Chair: Theodor Krauthammer
Major: Civil Engineering

In the past few decades, many studies have shown an increase in the nominal strength at failure of vary type of materials when subjected to high-loading or high-strain rates. The main explanation is believed to be the inertial forces that resist the displacement of the mass in the dynamic domain. This study examines the rate-effect phenomenon in a cylinder subjected to impact. A mass-spring system model, a finite element model, and previous tests results were used to analyze the problem. The main observation from these tests was that the specimens have remaining energy after the failure occurred, which presents itself as the kinetic energy of the fragments, several planes of failure, sound energy, etc. Both theoretical models showed an increase in the strain energy after the load stopped due to accumulated kinetic energy in the system. From those observations, it can be concluded that the energy which was applied to the specimen was greater than the energy needed to fail it, and therefore, the increase in the nominal strength at failure should be reexamined. This study suggests an alternate failure criterion, which is based only on the total amount of energy in the system and the amount of energy that will cause the specimen to fail.

CHAPTER 1
INTRODUCTION

Problem Statement

Concrete structures have traditionally been designed on the basis of strength criteria. This implies that geometrically similar structures of different sizes or structures subjected to different load rates should fail at the same nominal stress. However, in the past few decades, many studies have shown that the behavior of concrete under dynamic loading depends on the specimen size and loading rate. From experimental observations, a significant strength increase can be shown when concrete is subjected to high strain rates. This phenomenon has been called the strain rate effect and the strain rate sensitivity of concrete has become an important issue when impact loading is involved. In dynamic problems, the inertial force corresponds to the acceleration of the mass, and has significantly contributed to the force equilibrium. While in static cases $\Sigma F = 0$, in the dynamic case it becomes $\Sigma F = Ma$ or $\Sigma F - Ma = 0$. Thus, a material reaches its nominal failure strength at a higher load than the static critical load due to negative inertial force. This implies that a dynamic failure criterion should be formulated with respect to the inertia force to explain the rate effect. Many crack criteria for static problems have been proposed based on Linear and Non linear Fracture Mechanics to explain size effect, but only a few dynamic crack criteria have been proposed. A dynamic failure criterion is developed to predict the possibility of failure when a specimen is subjected to dynamic loading. The dynamic criterion can be superposed to the static crack criterion that explains the size effect. This practice may give reliable structural analysis results at high loading rates.

Research Significance

Concrete structures are designed and analyzed based on the strength of a standard laboratory-size specimen and based on a specimen subjected to a static load. Actual structures are much larger than the tested specimen and the actual concrete strength may be significantly lower than that of the standard size. Due to the neglect of the size effect, the predicted load capacity values become much less conservative in large structures. In addition, in the dynamic domain, specimens seemed to show higher strength as the load rate increased. Concrete structures can be subjected to high loading rates, such as those associated with impact, explosion incidents, etc. Those inaccuracies when testing different sizes and loading rates imply that nominal stress at failure depends on material properties, structural geometry and loading parameters. Thus, the relationship between properties, size, and loading parameters must be understood in order to predict the capacity values of a structure. The size effect is a phenomenon explained by the combination of plasticity and fracture mechanics, and it is related to the energy balance during the fracture process. The rate effect may be explained by the additional inertia force. In recent years, major advances have been made in understanding the size effect in the static domain and only a few studies have addressed the effect of higher loading rates on the size effect. If the structural strength can be defined as a function of material properties, dimensions and mass, more reliable analyses can be obtained.

Objective and Scope

The objective of this study is to develop a dynamic failure criterion for cylinders subjected to different compressive load rates. The theory of elasticity, the theory of waves, and energy method will be adopted to develop the criterion of failure for split

failure in a cylindrical specimen under compressive dynamic loading. This study assumes, material inertial effect is the primary cause of the strain-rate effect and concrete is failing in tensile strain. In the test of Krauthammer and Elfahal (2002), varieties of experiences were documented by data and high speed photographer camera. Based on that, this study on the one hand follows the failure mechanism, and on the other hand, verifies the expected results from the new criterion. Parallel computational simulations will also be used to track the failure and to verify the results from a numerical point of view. The study will focus on the Poisson effect mechanism of failure under compression, and the cylindrical specimen will be examined with respect to the failure mechanism.

CHAPTER 2
LITERATURE REVIEW

Overview of Current Literature

In the past few decades, many studies have shown that the behavior of concrete under dynamic loading depends on the specimen size and loading rate, contradicting the common assumption that strength is independent of the size and the rate of loading. In other words, it has been verified in those studies that the material properties of the specimens in the lab are not accurate enough and the results from the specimen test must be considered the influence of the actual structure size and the loading rate. There are two primary types of criteria when a failure is described, strain or strength based failure criteria and crack criteria. In the first criteria, the material failure is expressed in terms of stress or strain, and the size and rate effect are not taken into account. On the other hand, the crack criteria, based on fracture mechanics, and a governing equation are used to determine the crack propagation in terms of energy release rate. The basic concept of fracture mechanics is that the crack starts to propagate when the energy rate that is required for creating new crack surfaces is equal to the energy release rate. If the size and rate effect need to be considered, the mass must be included in the failure criteria like in the crack criteria. For size effect, there is an obvious connection between the size and the mass of the structure. For rate effect, the connection to the mass is with the inertial force that is included in the dynamic case.

Another approach may be introduced to analyze the rate effect is by wave propagation for the dynamic domain instead of analyzing the crack because the rapidly applied force is transferred to each particle of the mass on the path that the wave tracks. If the dimensions of the body are large, the time taken by the waves to traverse

the body becomes important. This propagation can be analyzed by two various compression tests one being the hammer test and second split-Hopkinson pressure test. The rate effect phenomenon is captured by both of these methods when experimenting with various load/strain rates.

Strain or Strength Based Failure Criteria

Most engineering materials can be categorized, based on their strain-strength response, into brittle, ductile or quasi-brittle, as shown in Fig. 2-1. In the case of a ductile material, a structure fails only when a nominal stress on the entire critical cross section reaches the material yield strength. In contrast, a perfectly brittle material fails whenever the maximum stress is equal to the tensile strength of the material. In between, a quasi-brittle material is characterized by a gradually decreasing stress after reaching the peak stress.

Concept of Fracture Mechanics

Fracture mechanics is the study of the response and failure of structures as a consequence of crack initiation and propagation. There are three fundamental modes of fracture: (I) opening, (II) sliding, and (III) tearing. Mode I is defined as a crack that is subjected to a tensile stress normal to the plane of the crack, mode II is defined as a crack that shear stress is acting upon, parallel to the plane of the crack and perpendicular to the crack front, and mode III is defined as a crack that the shear stress is acting upon parallel to the plane of the crack and parallel to the crack front as shown in Fig 2-2. For the purposes of this research only fracture in Mode I will be analyzed since when the compression load is applied to a concrete uniaxially, tensile strain is manifested in the lateral direction. In many cases, a single crack would grow to a critical length and then propagate in an unstable manner to complete failure. Most materials

contain some initial defects the propagation of which results in the failure of a structure. Fig. 2-3 represents an infinitely wide plate with an elliptical hole in the middle, submitted to a uniform tension. From an elastic stress analysis, the influence of the hole is obtained as (Shah, Swartz, & Ouyang, 1995)

$$\sigma_{max} = (1 + \frac{2a_1}{a_2})\sigma_N \quad (2\text{-}1)$$

where σN is the applied stress, σmax is the maximum stress along the edge of the hole, and a1 and a2 are the long and short radii of the ellipse, respectively.

It is seen from Eq. 2-1 that σ_{max} approaches infinity as the ellipse narrows. This fact indicates that no matter the magnitude of the load that is applied, the stress at a sharp crack tip reaches infinity, and the crack will propagate anyway. The above example indicates that neither elastic strain nor strength-based failure criteria can account for a sharp crack. The failure process for a brittle or quasi-brittle material with defects should be based on energy criteria. The energy criteria for failure of structures can be established using principles of linear elastic or nonlinear fracture mechanics.

Linear Elastic Fracture Mechanics

Griffith(1920) proposed energy failure criteria for ideally brittle materials that examined the change in energy due to the extension of a unit area crack, as shown in Eq. 2-2, and found the minimum required energy for a unit crack extension by setting the first derivative of Eq. 2-2 ,with respect to a, equal to zero. The result is shown in Eq. 2-3.

$$U - U_0 = -U_a + U_s \quad (2\text{-}2)$$

$$\frac{\pi a \sigma^2}{E} = 2\gamma_s \quad (2\text{-}3)$$

where U_0 is the initial elastic energy of the plate, U is the elastic energy of the cracked plate, U_a is the change in strain energy, which is equal to $\frac{\pi a^2 \sigma^2}{E}$ (Inglis, 1913), and U_s is the change in the elastic surface energy, which is equal to $4a\gamma_s$.

The energy release rate concept proposed by Griffith can be generalized by introducing the strain energy release rate for crack propagation (Surenda, Stuart, & Ouyang, 1995)

$$\Pi = U - F + W \tag{2-4}$$

$$\frac{\partial}{\partial a}(F - U) = \frac{\partial W}{\partial a} \tag{2-5}$$

where Π is the total potential energy, F is the work done by applied force, U is the strain energy of the structure, and W is the energy for crack formation. The right side of Eq. 2-5 represents the strain energy release rate per unit length of crack propagation, G, and the left side represents the critical strain energy release rate, G_c. Eq. 2-5 can be written as

$$G = G_c \tag{2-6}$$

Nonlinear Fracture Mechanics

The same principles of strain energy release rate that have been demonstrated in the previous section for LEFM can be used for NLFM. In a linear elastic (brittle) material, any propagation of a crack means catastrophic failure of the material. However, in a nonlinear material, a crack may steadily propagate until it reaches a critical length. As in LEFM, the energy release rate must be equal to the fracture resistance of the material during crack propagation. In nonlinear materials, propagation of a crack may be stable, stationary, or unstable because of the presence of crack

arrest mechanisms in the inelastic zone around the crack tip. The stable crack means that the crack propagates only when applied load or displacement increases, whereas in the unstable crack, the crack may propagate even though the applied load decreases or keeps constant. The stationary crack propagation is a critical state between stable and unstable crack growth, as illustrated in Fig. 2-4. The equilibrium for stable, stationary, and unstable crack growth can be defined by the derivative of Π with respect to the crack length, a, instead of x, where Π is the total potential energy, as mentioned in Eq. 2-5.

MLFM for Mode I Crack in Concrete

There are two principal features that control the mechanical behavior of concrete. One, concrete is very weak in tension, about 10% of its compressive strength. The second is that many internal flaws and cracks exist prior to loading. The fracture process zone is the inelastic zone around the crack tip in which the internal cracks and flaws propagate. The energy release rate for quasi-brittle material, Gq, composed of two portions (Shah, Swartz, & Ouyang, 1995), is represented by

$$G_q = G_{Ic} + G_\sigma \tag{2-7}$$

where GIc is the material surface energy rate, and Gσ is the energy rate to overcome the cohesive pressure σ(w) in separating the surfaces, as shown in Fig. 2-5 and defined in Eq. 2-15

$$G_\sigma = \int_0^{w_t} \sigma(w)dw \tag{2-8}$$

Propagation of Waves in Elastic Solid Media

Timoshenko and Goodier (1951) noticed the difference between the static case and the dynamic case, and their solution based on the concept of propagation of waves.

The main difference is that the action of a suddenly applied force is not transmitted at once to all parts of the body, and deformations produced by the force are propagated through the body in the form of elastic waves. If the dimensions of the body are large, the time taken by the waves to traverse the body becomes important. They presented the following two velocity equations

$$c = \sqrt{\frac{E}{\rho}} \tag{2-9}$$

$$v = \frac{\sigma}{\sqrt{E\rho}} \tag{2-10}$$

where c and v are the stress propagation wave velocity through the material and the velocity given to the particles in the affected zone by the stress wave, respectively.

In their study, two cases of traveling waves are presented, one being when a wave meets the free end of a bar and the other being when a wave meets a fixed end. In the first case, a compressive wave is reflected as a similar tension wave, and vice versa. In contrast, in the second case, a wave is reflected from a fixed end entirely unchanged.

The wave propagation and the velocities c and v may be explained by considering two equal bars of the same material striking each other longitudinally with the same velocity v, as shown in Fig. 2-6. Assuming that the contact takes place at the same instant over the whole surface of the ends of the bars, the progress of the events during the impact will take place as follows: The plane of the contact, mn, will not move during the impact, and two identical compression waves will start to travel along the bar, away from plane mn with equal velocities c. The velocities of the particles in the wave are equal to v with direction away from the contact plane, superposed on the initial velocities of the bars, bring the zones of waves to rest, and when the waves reach the

free ends of the bars, both bars at this phase are uniformly compressed and at rest. Based on the understanding above, the compression waves will be reflected from the free end bar as similar tension waves with velocity equal to c with direction toward the cross section of the contact mn. The velocity of the particles in these waves will now be equal to v (the bars' velocities are zero), with direction away from mn because the waves will be in tension. When the waves reach mn, the bars separate with a velocity equal to their initial velocity v with the opposite direction. The duration of the impact in this case is equal to the time that takes the wave to propagate back and forth in the beam, which equal to $2l/c$. The compressive stress in the bar is equal to $\sigma = \nu\sqrt{E\rho}$, from Eq. 2-10.

A more complicated example (Timoshenko & Goodier, Theory of elasticity, 1951) (Timoshenko, Vibration problems in Engineering, 1937) is presented in Fig 2-7, where a bar with a fixed end is hit by a moving mass at the other end. M and v_0 are the mass of the hitting body per unit of the cross section of the bar and the initial velocity of the body, respectively. Let t=0 be defined as the instant of impact; at this time $\sigma_0 = \nu_0\sqrt{E\rho}$, From Eq. 2-10. Owing to the bar resistance, the velocity of the moving body and so the compressive stress in the contact cross section of the bar will gradually decrease, as shown in Fig. 2-7 (b). During this phase, a compression wave with a decreasing compressive stress travels along the length of the bar. In the case of a fixed end, when the wave reaches the end of the beam it is reflected without change toward the contact section. The velocity of the hitting body cannot change suddenly, so the wave will be reflected again as from a fixed end and will continue traveling away from the contact area. At the surface of contact, when the wave is moving away, the compressive stress

suddenly increases by $2\sigma_0$, as can be seen in Fig. 2-7 (c). Such a sudden increase occurs during impact at the end of every interval of time, $T = 2l/c$, the time it takes the wave go back and forth in the beam. The general expressions for the total compressive stress and the velocity of particles at the end struck during any interval $nT < t < (n+1)T$ are (Timoshenko & Goodier, 1951)

$$\sigma = S_n(t) + S_{n-1}(t - T) \tag{2-11}$$

$$v = \frac{1}{\sqrt{E\rho}}[S_n(t) + S_{n-1}(t - T)] \tag{2-12}$$

where $S_n(t)$ is the total compressive stress produced at the end struck by all waves moving away from this end.

Rate Effect

A significant strength increase can be observed when concrete is subjected to high strain rate. This phenomenon is called the strain rate effect, as can be seen in Fig 2-8. In this figure the results were obtained by the split Hopkinson compression bar test as will be explained in the following section in detail. The strain rate sensitivity has become an important issue when impact loading is involved. It can be seen in Fig. 2-8 that two areas with different strain-strength increase rates can be distinguished. The first area, corresponding to strain rates between 10^{-6}(s^{-1}) and 10 (s^{-1}) leads to a strength increase of about 150%. On the other hand, the strength enhancement corresponding to strain rates higher than 10 (s^{-1}) is much steeper. Viscosity related to the presence of water in the pores of the concrete (Rossi, 1991) and a crack path through harder aggregates (Chandra & Krauthammer, 1995) are proposed as the main causes of the

strength increase in the low strain rates. In the second area, involvement of the inertial forces may explain the steep increase (Weerheijm, 1992).

Chandra and Krauthammer (1995) showed, as an explanation of the rate effect, the influence of inertial force in a dynamic domain by using a mass-spring system, as follows: a lumped mass, M, and a linear spring of stiffness, K, as can be seen in Fig. 2-9(a), is subjected to a dynamic force, P(t), as can be seen in Fig. 2-9(b), varying with time, t, given by

$$P(t) = \alpha t \tag{2-13}$$

where α is the loading rate.

The governing equation of motion is

$$M\ddot{x} + Kx = P(t) \tag{2-14}$$

and the solution is

$$x = \frac{\alpha}{K}\left(t - \frac{1}{\omega}\sin\omega t\right)$$
$$\omega = \sqrt{\frac{K}{M}} \tag{2-15}$$

where x is the displacement of the mass.

So the internal force in the spring can be expressed as

$$Fs = Kx = \alpha t - \frac{\alpha \sin\omega t}{\omega} = P(t) - \frac{\alpha \sin\omega t}{\omega} \tag{2-16}$$

Eq. 2-16 expresses the internal force in the spring, Fs, which is smaller than the external force, P(t), because of the influence of the inertial force of the mass, $\frac{\alpha \sin\omega t}{\omega}$, as

can be seen in Fig. 2-9(c). So a material reaches its nominal failure strength at a higher load than the static critical load due to negative inertial force.

Suaris and Shah(1981) proposed using a rubber pad between the striker and the specimen in order to minimize the inertia effect so that one can obtain an objective dynamic concrete strength. Using the LEFM, Weerheijm(1992) developed a rate-sensitive fictitious fracture plane model by adding kinetic energy to the energy failure criteria. Weerheijm showed the capability of the model to predict the rate effect under tensile strength. John and Shah(1986) performed several tests on single-edge notched beams with a gauge that measures the propagation of a single continuous surface crack (KRAK gauge), and showed that the amount of pre-peak crack growth decreases with the increase in loading rate. That observation may indicate that the fracture process zone decreases at high strain rates, hence, LEFM may be valid.

Split Hopkinson Bar Method

The split Hopkinson test was introduced by Bertram Hopkinson in 1914 in order to measure stress pulse propagation in a metal bar. Although this method is one of the most common techniques to measure material properties at high stresses, in this work no such experiment was applied; however, suggested for more detailed research in the future. The experimental setup consists of a striker bar along with a specimen sandwiched between an incident bar and a transmission bar as seen in Fig. 2-10. The bars are typically made out of high strength steel with diameters of 0.75 inches and a length of approximately 5 feet.

To conduct the experiment the striker bar is fired to achieve a certain speed and hit the pulse shaper, which in turn creates a stress wave that propagates through the pulse shaper to the transmission bar. This incidence stress wave is split into two smaller

parts commonly named transmitted and reflected waves. The transmitted wave is what causes the plastic deformation in the specimen while the reflected wave, as the name suggests, reverts from the specimen and travels back toward the incident bar. The strain gages transmit all the deformation history to a computer to be analyzed.

To analyze the data, the specimen stress is calculated implementing the Kolsky relation that is given in the following equation (Kolsky, 1949) where E represents the output pressure bar's elastic modulus, A_0 indicates the sample's cross sectional area, and $\varepsilon_T(t)$ is the transmitted strain history:

$$\sigma_s(t) = E\frac{A_0}{A}\varepsilon_T(t) \tag{2-17}$$

Then the specimen strain rate is calculated from the following formula where $\varepsilon_R(t)$ is the reflected input bar strain history, L is the specimen length before impact, and C_0 is the infinite wavelength wave velocity in the incident bar calculated from elementary vibrations as the square root ratio of E(elastic modulus) and ρ (density) of the bar:

$$\frac{d\varepsilon_s(t)}{dt} = -\frac{2C_0}{L}\varepsilon_R(t) \tag{2-18}$$

Finally, combining the equations above yields the specimen's strain that may be expressed as:

$$\varepsilon_s(t) = -\frac{2C_0}{L}\int_0^t \varepsilon_R(t)dt \tag{2-19}$$

Since the relationship between stress and strain is achieved, the external stress applied to the strain presented in the specimen can be computed; thereby, new stress strain curves can be analyzed for various strain rates.

Drop Hammer Test Method

Another method to measure the stress-strain relationship in a compression test is to apply the drop hammer test, in which the rate effect observed is in the dynamic domain. A typical hammer use for the test is shown in Fig. 2-11. After the weight and height are set to get the desirable load, the hammer is dropped to collide with cylinder and the loads are captured by load-cells located at the bottom of the hitting body while the strains are captured by the strain-gauges that are located on the longitudinal direction of the cylinder. The load cells measure the external load applied and the strain gauges measure the strain corresponds only to the internal force.

Drop Hammer Test Method versus Strip Hopkinson Bar Test

In both tests two types of velocity is introduced one being the velocity of the wave and the second the velocity of the mass particle. Wave velocities are dependent on the material properties while the mass particles' velocity depends on stress that applied on the incident bar. The strain data is acquired from strain gauges at various locations; therefore, the time for the load wave propagation is important. In the drop hammer test the energy is dissipated only in the specimen; however, in the split Hopkinson test the energy travels between the incident bar and transmission bar. Split Hopkinson bar test measures different strain rates while in the drop hammer test the load rate is obtained by the velocity of the hammer. For this research all the data was gathered out of 127 drop hammer tests with various load rates.

Size Effect in Concrete

The classical definition of size effect may be phrased as the dependence of the nominal stress at failure of the concrete on its characteristic dimension. This implies that specimens of different sizes fail at different nominal stresses, despite the fact that they

are made from the same material and they are geometrically similar. The existence of size effect in concrete has been well established through many studies, experimental as well as theoretical. The most important theory on the source of size effect is the fracture mechanics size effect theory. According to the theory, size effect is caused by the release of stored energy in the structure into the fracture front. Kazemi & Bazant (1991) proposed a size-dependent nominal strength, σ_n, of geometrically similar structures, called the Size Effect law

$$\sigma_N = \frac{B_0 f_t}{\sqrt{1 + \frac{D}{D_0}}} \tag{2-20}$$

where B_0 and D_0 are constant empirical parameters dependent on material properties and structural shape, f_t is the size independent tensile strength of the material, and D is the characteristic dimension of the structure.

Fig. 2-12 shows the smooth curve of the NLFM that is presented by Eq. 2-20. It can be seen that the nominal strength of the strength criterion is constant as predicted because it is a criterion independent of size, and it may only be used for relatively small-sized structures (Baznat & Planas, 1998). The LEFM predicts a linear change for the nominal strength because it is a single-parameter failure criterion and is true for relatively large structures, where D_o may be defined as the limit between the two.

In the dynamic domain, the concept of size effect has not been studied extensively, and its behavior under short-duration dynamic loading, such as impact or earthquake, has not been studied enough (Krauthammer & Elfahal, 2002). Some available data show a relationship between loading rate and size effect (Lessard,

Challal, & Aiticin, 1993). However, when compared to impact loading rate, the loading rates from the available data are considered low.

Coupled Size and Rate Effect

A recent study presented by Park and Krauthammer(2006) showed an energy criterion containing a component of kinetic energy, based on Griffith and LEFM theories. This dynamic energy criterion implies that the applied energy rate should be equal to the sum of changes in the strain, kinetic, and fracture energies

$$\dot{U}_e = \dot{U}_s + \dot{U}_k + 2\gamma B\dot{a} \tag{2-21}$$

where U_e, U_s, and U_k are the external, strain, and kinetic energies, respectively, B is the specimen width, and γ is the surface energy required for a crack to propagate through a given area. For a simplified model with a mass, M, connected to a spring with spring constant, K, as shown in Fig. 2-13, the energy rate terms can be formulated as follows (Park & Krauthammer, 2006)

$$\dot{U}_e = \frac{d}{dt}(Pu) = P\dot{u} \tag{2-22}$$

$$\dot{U}_s = \frac{d}{dt}\left(\frac{1}{2}K(a)u(t)^2\right) = Ku\dot{u} + \frac{1}{2}\frac{dK}{da}u^2\dot{a} \tag{2-23}$$

$$\dot{U}_k = \frac{d}{dt}\left(\frac{1}{2}M(a)\dot{u}(t)^2\right) = M\ddot{u}\dot{u} + \frac{1}{2}\frac{dM}{da}\dot{u}^2\dot{a} \tag{2-24}$$

Based on equilibrium of motion, P is also equal to

$$M(a)\ddot{u} + Ku = M\ddot{u} + \frac{dM}{da}\dot{a}\dot{u} + Ku = P \tag{2-25}$$

By combining Eq. 2-21, 22, 23, and 24 with Eq. 2-25, the energy flow can be expressed as

$$2\gamma B\dot{a} = \left[-\frac{1}{2}\frac{dK}{da}u^2 + \frac{1}{2}\frac{dM}{da}\dot{u}^2\right]\dot{a} \tag{2-26}$$

where the left side of Eq. 2-26 represents the energy required for a crack to propagate, and the right side represents the energy released from the specimen when a crack propagates. So, the LEFM dynamic crack criterion can be defined as

$$2\gamma = \frac{1}{B}\left[-\frac{1}{2}\frac{dK}{da}u^2 + \frac{1}{2}\frac{dM}{da}\dot{u}^2\right] \tag{2-27}$$

where a crack cannot propagate if the right side of Eq. 2-27 is less than the left side. The component involved with the mass in Eq. 2-27 is the addition for the dynamic case, and because of this additional component, a strength enhancement is expected. Thus, Eq. 2-27 expresses both size and rate effect.

In the experimental area, a comprehensive study presented by Krauthammer and Elfahal (2002) examined four different sizes of geometrically similar high-strength and normal-strength concrete cylinders under both dynamic and static loading. In addition to the specimens, simulation models in ABAQUS were used. Some of the tests were recorded using high-speed photography. This study showed the following:

- The size effect existed for compressively loaded high-strength and normal-strength concrete cylinders under both static and dynamic loads.
- The size effect law predictions were proved to match the static test results for both the high-strength concrete and the normal-strength concrete specimens with the change of specimen sizes.
- Higher loading rates were found to enhance the apparent strength of both the normal and high-strength concrete specimens.
- Use of high-speed photography enabled the detection of many modes of failure of concrete specimens under dynamic tests. Generally, large and stronger specimens tend to fail in a brittle manner while smaller and softer specimen fail in a manner similar to that observed in static test.
- The modes of failure were labeled into seven principal shapes, as followes:

- Vertical splitting: the cylinder split vertically through two, three or more vertical planes, as shown in Fig. 2-14 (a), (b), and can start either at the top or at the bottom, as shown in Fig. 2-14 (c) and (d), respectively.
- Cone-shaped shear failure: an hour glass shape similar to the static failure, as shown in Fig. 2-14 (e)
- Diagonal shear failure: a diagonal failure plane, as shown in Fig. 2-14 (f), and in some cases it occurring in combination with vertical splitting. In some other cases shear failure occurred in combination with shell bursting as can be seen in Fig. 2-14 (g)
- Buckling failure: this mode of failure was distinguished by the inflation of the cylinder from the bottom or the top, as shown in Fig. 2-14 (h) and (i), respectively.
- Compressive belly failure: similar to a belly shape, the inflation occurred in the center, as shown in Fig. 2.14 (j).
- Shell-core failure: this mode was distinguished by bursting of the shell of the cylinder leaving a core at the center, as can be seen in Fig. 2-14 (k).
- Progressive collapse: a gradual transfer of failure from the top to the bottom of cylinder as the hammer went deeper down inside the cylinder, as can be seen in Fig. 2-14 (l),(m). The uniqueness of this failure is that the specimen stands intact in place while the hammer is moving down and progressively eroding the specimen from the top.

Another experimental study (Zhang, Ruiz, & Yu, 2008) presents very recent test results of similar geometrical reinforced concrete beams of three different sizes under four strain rates. This study showed that the peak loads increase with an increase in the strain rate and are stronger for larger specimens than for smaller ones. On the other hand, the size effect is only shown under low strain rates and becomes inconspicuous in higher strain rates.

Finite Element Models

Finite element analysis is a numerical method to approximate the solutions for partial differential equations. To solve the problems these equations are either modified to be ordinary differential equations to be integrated utilizing various methods (eg. Euler,

Range-Kutta) or for steady state problems the differential equation is entirely eliminated. Because of the modern FEM, tools and structures can be analyzed for bending, twisting visualizing the stresses and the strains to allow redesigning, rendering, and/or optimizing the structure.

In the numerical simulation domain, many of the studies that were mentioned used an additional finite element model similar to the specimens of the test, and the results were compared to each other. Krauthammer and Elfahal (2002) performed finite element simulations before the experimental work and after. The aim of pre-test simulations aim was to help in assess the anticipated behavior, as well as to help design the test, and the post-test simulations aim was to improve the finite element models with respect to the results obtained in the experimental work in order to minimize the differences between the model and the test results. In that study, the finite element simulations were performed using the finite element code ABAQUS Explicit. The reported results showed that both post-test plasticity-based and fracture-based models succeeded in predicting the existence of size effect. It was recommended that the hitting body should be modeled with the same geometrical shape and size as that in the real test. Another recommendation was that according to the value of d_0, the plasticity-based model and the fracture-based model should be used for all specimens that lie in the plasticity region and fracture region of the size effect curve, respectively.

Zhou and Hao (2008) presented mesoscale modeling of concrete as a three-phase composite consisting of aggregate, mortar and interfacial transition zone (ITZ) between the aggregate and the mortar. The mesoscale model was adopted to analyze the dynamic tensile behavior of concrete at high strain rates. It was assumed that within

the ITZ area, the material properties are weaker than the mortar matrix. The strength criterion was governed by a damage-based yield strength surface, where the dynamic yield strain surface was amplified from the static surface by a dynamic factor that represents the strain rate effect. From the numerical results, it was found that the crack pattern and the tensile strength were highly affected by the aggregate distribution and the properties of the interfacial transition zone.

A common method used in ABAQUS to model concrete behavior is the concrete damage plasticity (CDP) model, which is a continuum that is elasticity-based model that account for concrete damage. The basic assumption is that concrete may fail under both compressive and tensile loads. Two stress-strain curves were used to define this behavior of the materials as seen in Fig. 2-15 and Fig. 2-16. The parameters seen in those figures are defined as the following:

E_0: elastic young modulus of undamaged concrete in the elastic range.

σ_{co}: initial yield stress

σ_{cu}: ultimate stress in the plastic range

σ_{to}: tensile failure stress

σ_c: concrete compressive stress

σ_t: concrete tension stress

d: damage parameter that ranges from zero (no damage) to one (total loss of strength)

d_c: damage parameter for compression

d_t: damage parameter for tension

ε_c^{in}: inelastic compressive strain

ε_{oc}^{el}: elastic compressive strain

ε_c: total compressive strain

ε_t^{ck}: cracking strain

ε_{ot}^{el}: elastic tension strain

ε_t: total tension strain

ABAQUS converts the inelastic strain values into plastic strain values automatically by utilizing the following equations:

$$\varepsilon_c^{pl} = \varepsilon_c^{in} - \left(\frac{d_c}{1-d_c}\right)\left(\frac{\sigma_c}{E_o}\right) \quad (2\text{-}28)$$

$$\varepsilon_t^{pl} = \varepsilon_t^{ck} - \left(\frac{d_t}{1-d_t}\right)\left(\frac{\sigma_t}{E_o}\right) \quad (2\text{-}29)$$

Summary

The rate effect is a very important phenomenon that define structural behavior under sever dynamic loads. This phenomenon was not understood well and was described by empirical equations. Solving the aforementioned problem will ensure more accurate structural analyses of critical facilities. The drop hammer test made by Krauthammer & Elfahal (2002) model showed rate effect in testing 127 cylinders with various load rates. In this research results from these tests will be examined when adopting Chandra & Krauthammer (1995) models to understand the influence of inertial force in the rate effect phenomenon. Different ideas in fracture mechanics will be implemented to develop the criterion of failure based on energy equations. Theory of wave propagation will be used to better understand the differences in the static and dynamic domains. To analyze the cylinder a finite element model will be chosen utilizing the computer software called, ABAQUS.

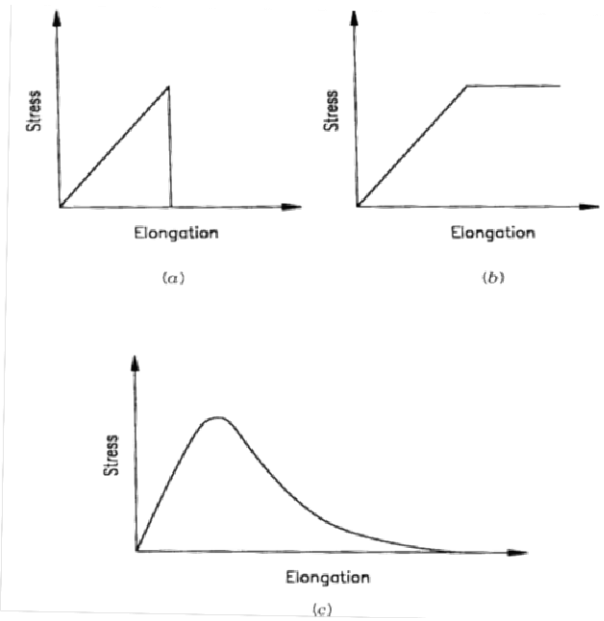

Figure 2-1. Different types of materials: (a) brittle material, (b) ductile material and (c) quasi-brittle material (Shah, Swartz, & Ouyang, 1995)

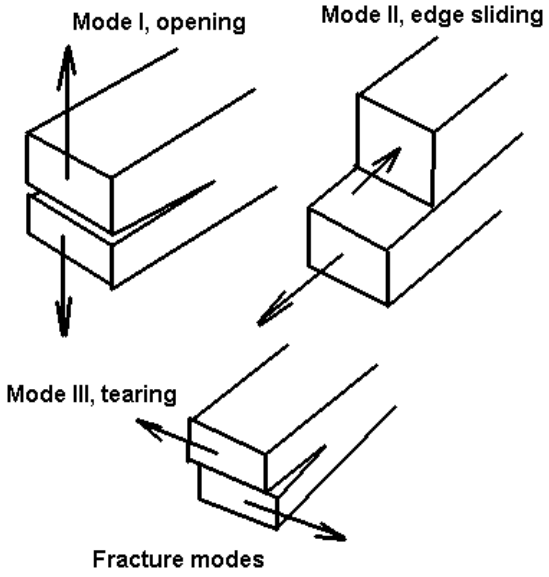

Figure 2-2. The three fundamental fracture modes of crack

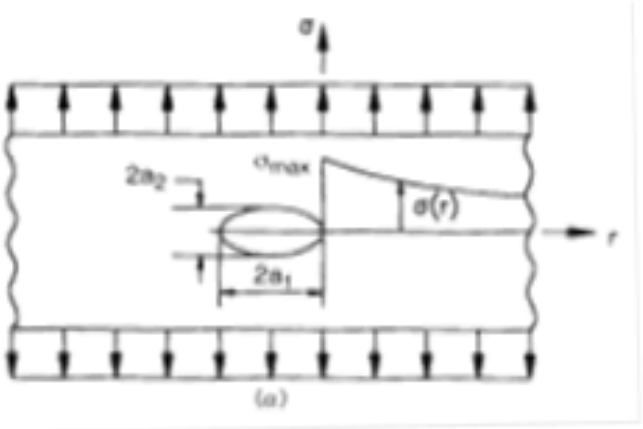

Figure 2-3. Distribution of internal stress in the region of an elliptical flaw in an infinitely wide plate (Shah, Swartz, & Ouyang, 1995)

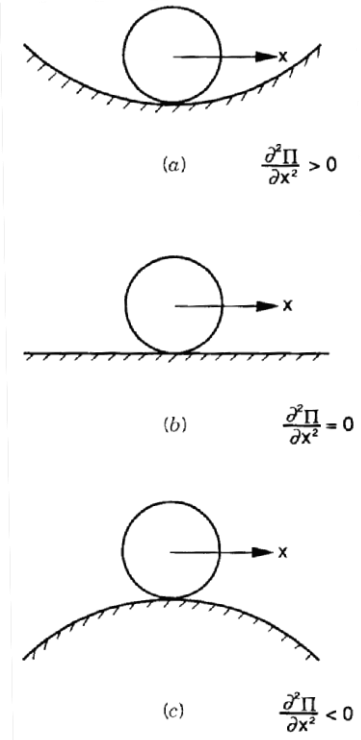

Figure 2-4. Illustration of different equilibrium states: (a) stable, (b) stationary, and (c) unstable equilibrium state (Shah, Swartz, & Ouyang, 1995)

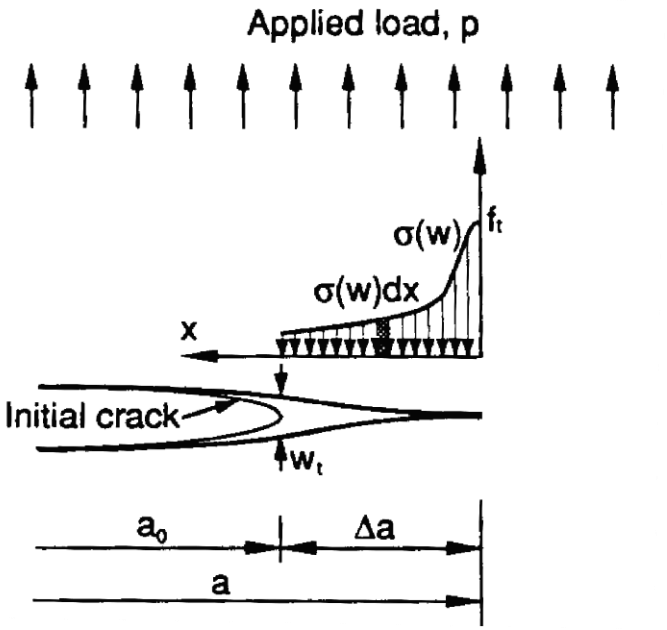

Figure 2-5. Modeling of quasi-brittle crack (Shah, Swartz, & Ouyang, 1995)

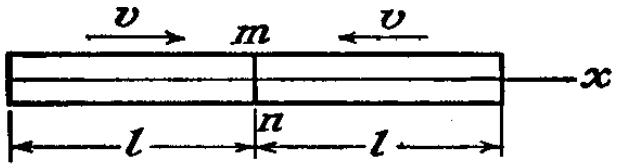

Figure 2-6. Impact between to bars (Timoshenko & Goodier, 1951)

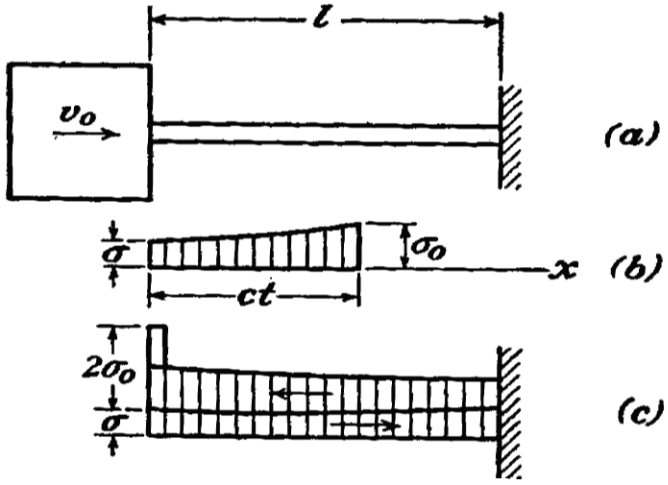

Figure 2-7. A bar hit by a moving mass (Timoshenko & Goodier, 1951)

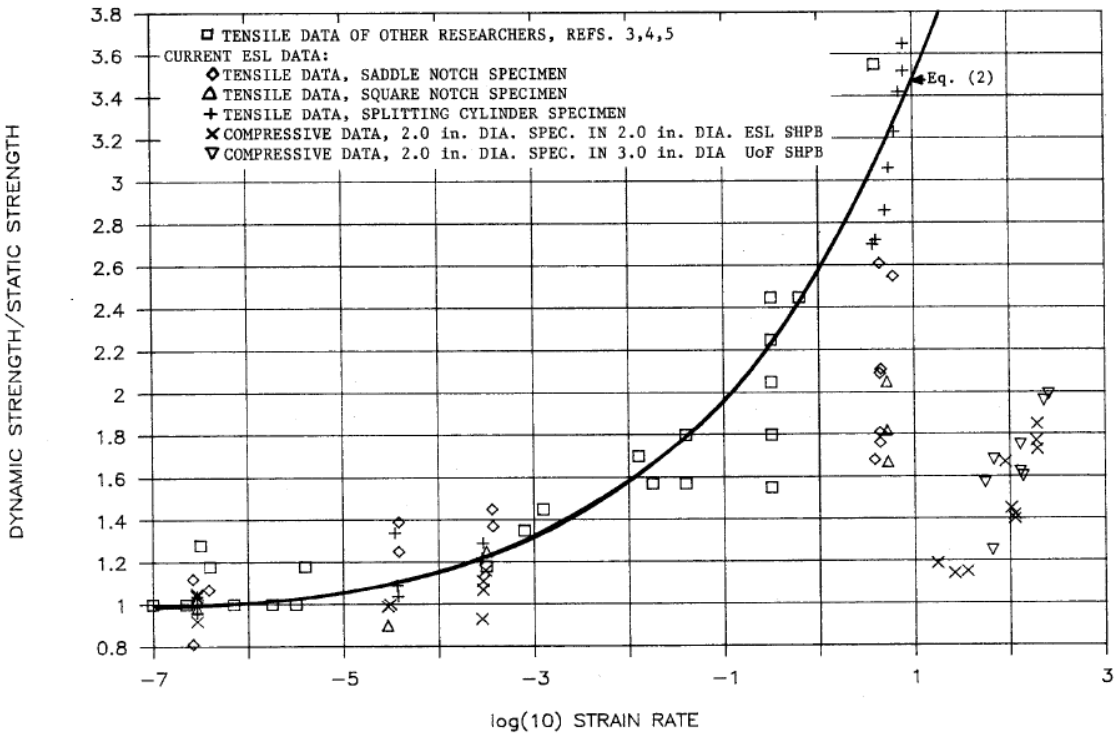

Figure 2-8. Effect of loading rate on compressive strength of concrete (Ross, Kuennen, & Strickland, 1989)

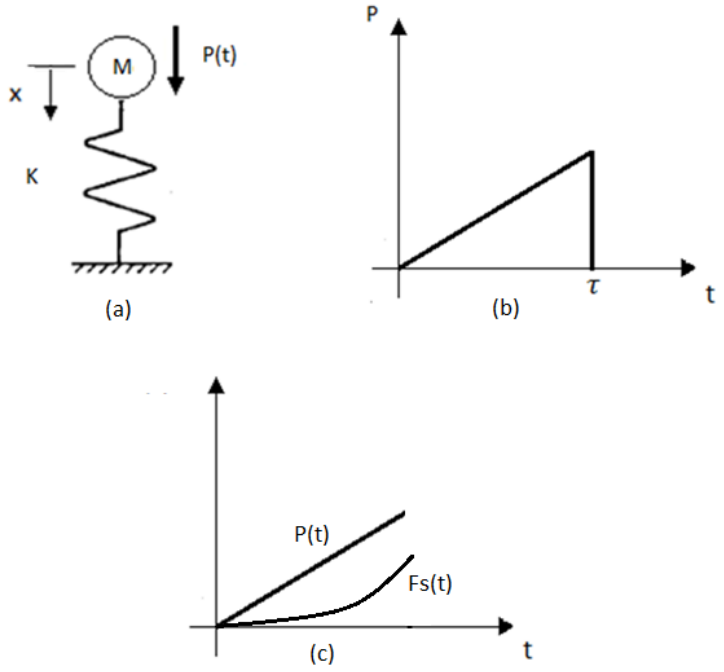

Figure 2-9. A mass-spring system analysis: (a) A mass-spring system, (b) Applied dynamic load, and (c) Internal force in spring

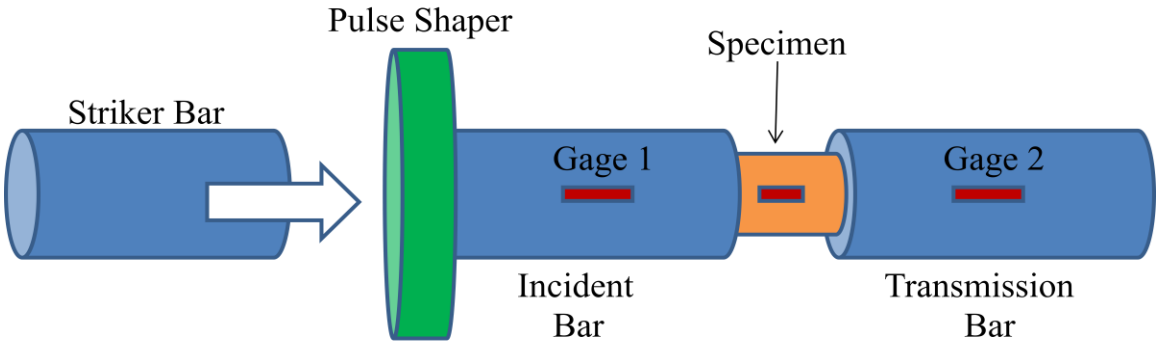

Figure 2-10. Split Hopkinson Pressure Bar (SHPB)

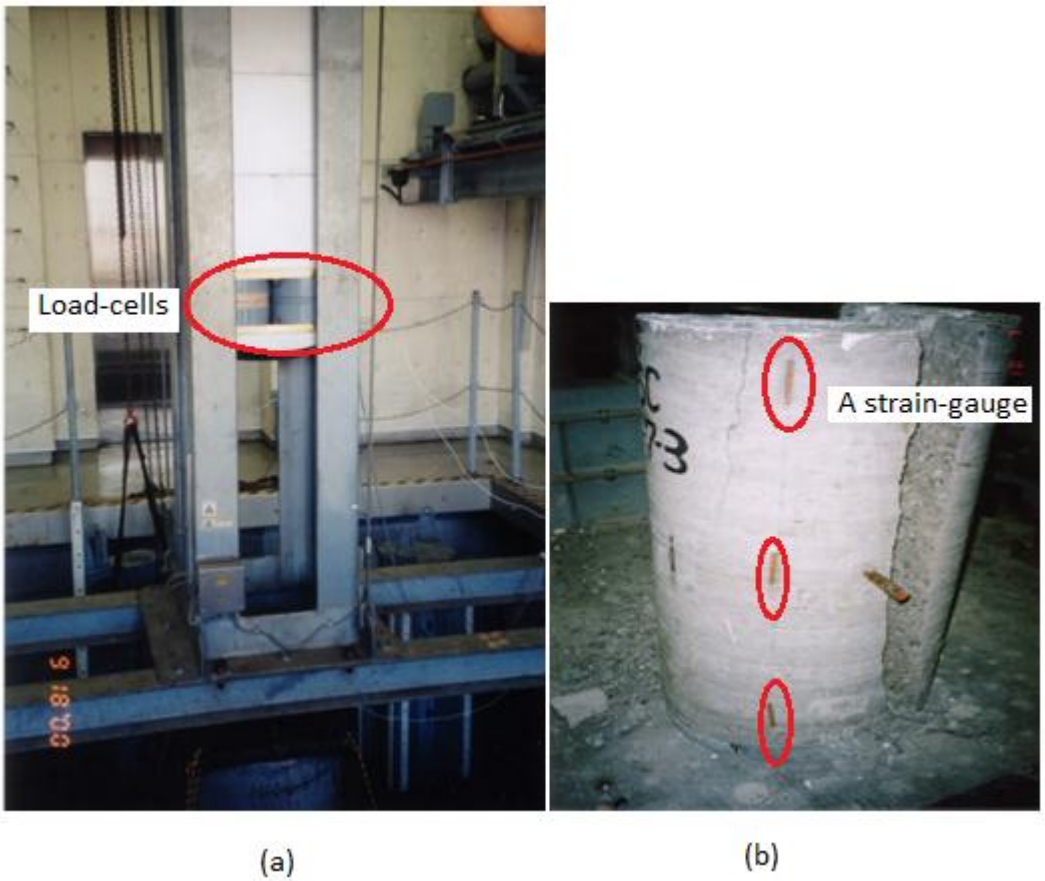

Figure 2-11. Drop Hammer Test: (a) A typical hammer and the load-cells, (b) Strain-gauges on a specimen

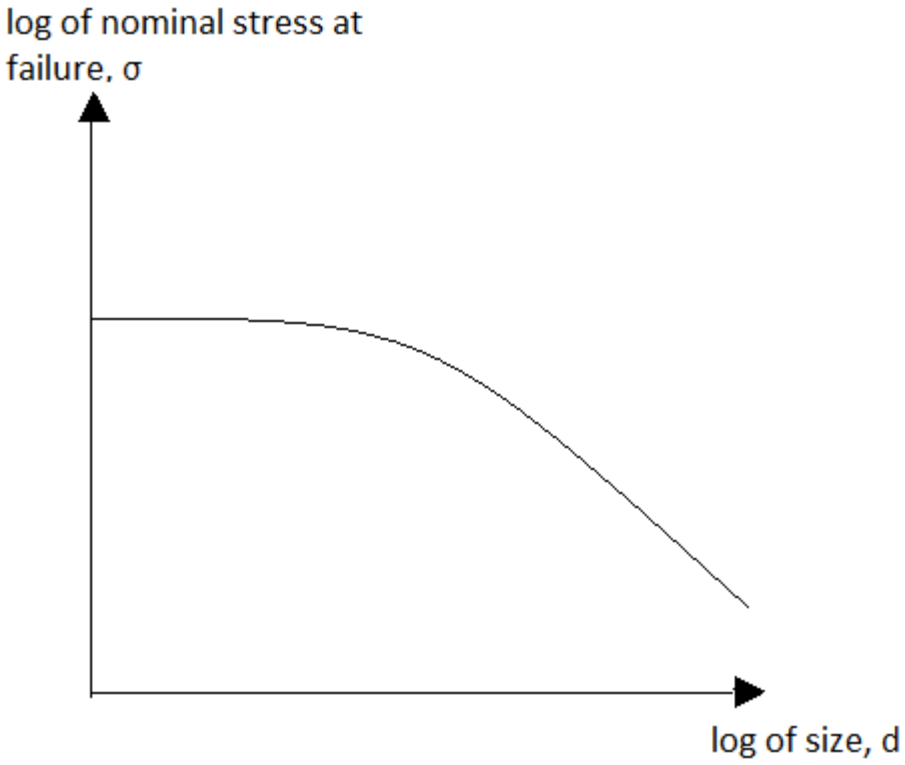

Figure 2-12. Size effect law

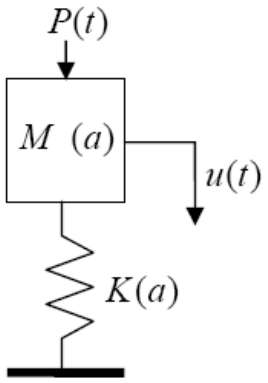

Figure 2-13. Simple dynamic mass and spring model

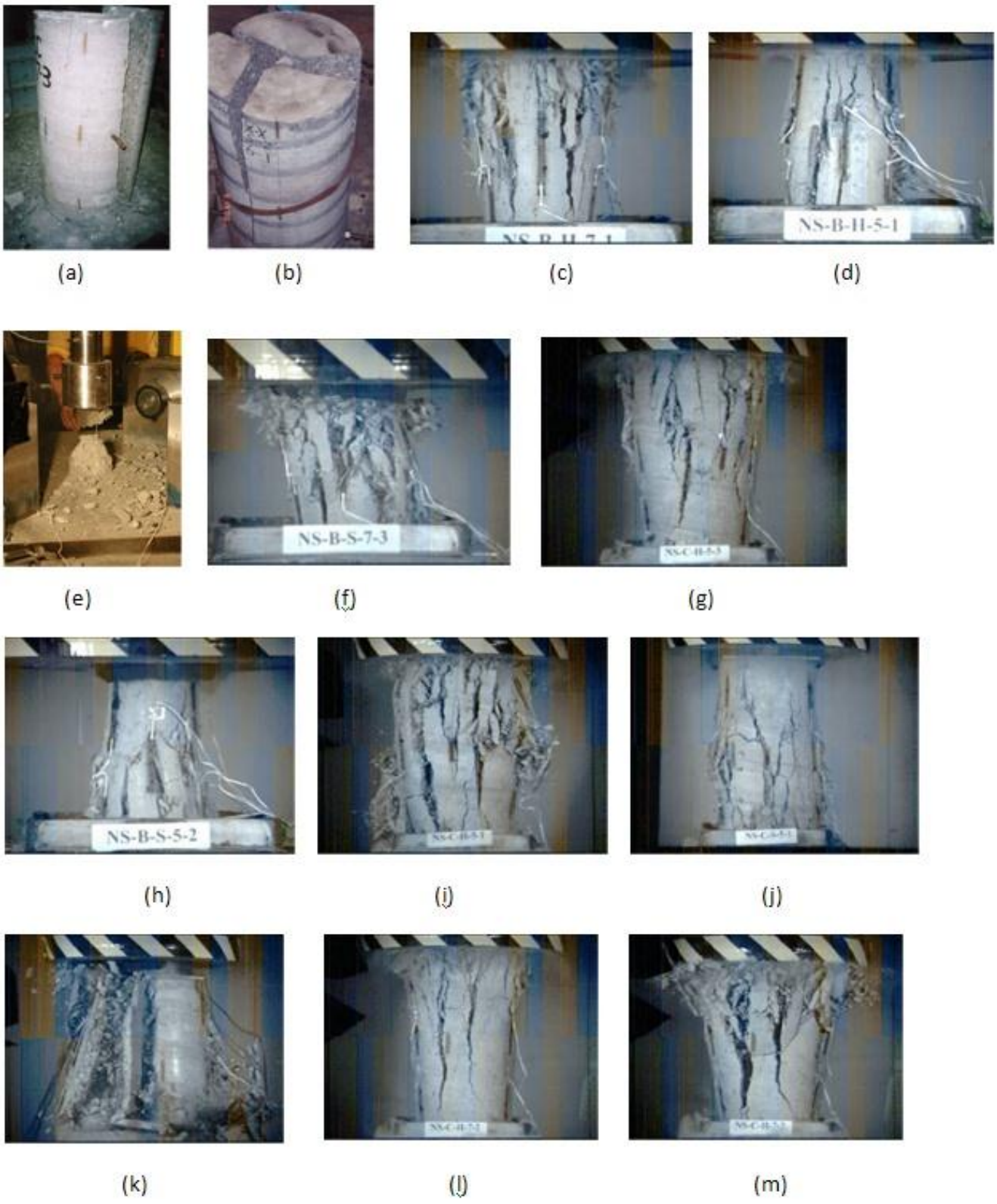

Figure 2-14. Modes of failure (Krauthammer & Elfhahal, 2002)

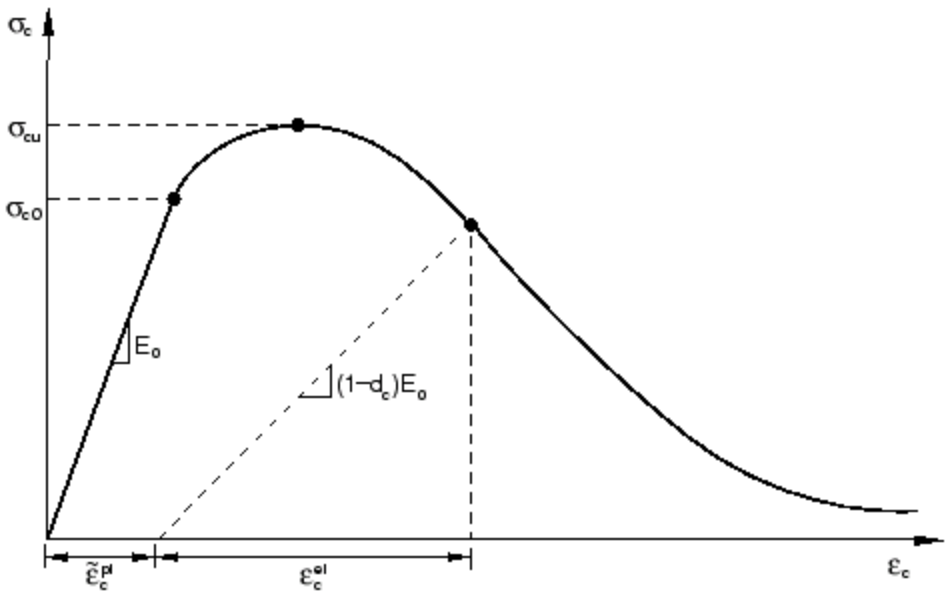

Figure 2-15. Compressive stress-strain curve in CDP model (Simulia, 2010)

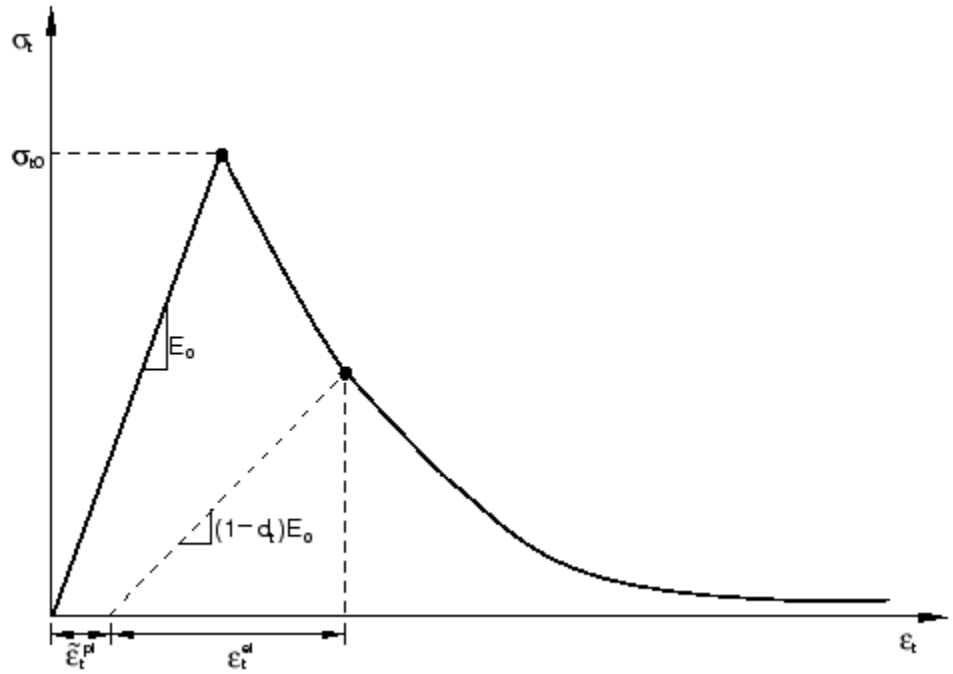

Figure 2-16. Tension stiffening stress-strain curve in CDP model (Simulia, 2010)

CHAPTER 3
METHODOLOGY

Research Approach

In Krauthammer and Elfahal's (2002) tests, the modes of failure were classified into seven principal shapes: vertical splitting, cone-shaped shear failure, diagonal shear failure, buckling failure, compressive belly failure, shell-core failure, and progressive collapse. This study examines the first principal shape, vertical splitting. In this principal shape, the Poisson effect is believed to be the characteristic that controls the failure process. In this characteristic of failure, the compressive load causes a compression strain in the direction of the load and a tensile strain in the lateral direction which fails the concrete in Mode I (opening mode as explained in the fracture mechanics section) when it reaches its maximum tensile strain. In the dynamic domain in addition to the strain, velocity and the mass particle are present in both directions: the velocity of the mass is in the longitudinal direction is due to the force applied, and in the transverse direction the velocity is due to the Poisson effect. The velocity of the mass causes inertial forces, which keep the crack from opening. In order to understand the mechanism of inertial force, the first step will be a mass-spring system with a lumped mass, M, and a linear spring of stiffness, K. As discussed in Section 2.8, the influence of the inertial force is the main cause to observe strain-rate effect, and as a result, a material reaches its nominal failure strength at a higher load than the static critical load. This study adopts the explanation above but suggests a reexamination of the conclusion. The mass has a non-zero velocity at failure which implies that the applied load was higher than the capacity of the specimen, so the observation of strengthening is questionable. This study suggests an approach based on equilibrium energy to

analyze the failure in the dynamic domain, in which the question to determine if the failure occurs or not should be: is the work done by the applied load more or less than the critical energy of the system?

A time-line is an important factor when the effect of high loading rates is examined. Two factors might vary with respect to time and should be observed over time: the applied load and the displacement of the mass. In order to use the energy method, a relation between the applied load and work done by the applied load with respect to time is developed. This study suggests that a P-I curve is the correct way of representing whether a failure occurs in the dynamic domain. Using the suggested approach, the nominal strength at failure can be found for various values of impulse, and a P-I curve can be developed. The second step is to use parallel computational simulations to examine the differences between the mass-spring system and a three-dimensional model with multiple degrees of freedom. In the final step, finite element models are used to obtain the amount of energy needed for the Poisson character of failure to appear.

Poisson Failure in a Cylinder

In the Krauthammer and Elfahal's (2002) tests, some of the cylinders split vertically through two, three or more vertical planes as a result of the Poisson effect, as can be seen in Fig. 3-1.

When a uniaxial compressive specimen is tested, some lateral restraint stress, shear stresses, may develop at the machine-specimen boundary due to different deformations between the steel loading plate and the concrete (Surenda, Stuart, & Ouyang, 1995). The stress state arrests cracking in the end regions, which may delay or prevent formation of cracks. Therefore, when testing a short specimen, a cone-shaped

mode is usually obtained, as can be seen in Fig. 3-1 (d). This type of failure mode cannot be used to characterize Poisson effect failure, and it seems to be an intermediate stage between the Poisson effect and Shear failure.

As mentioned before, this study adopts the explanation that the inertial force is the main cause to observe strain-rate effect. The inertial force causes a difference between what the external load applies and the actual load acts on the cylinder as will be described in the next section. The displacement of the cylinder corresponds to the load that the cylinder experiences and not to the external load. So when the external load is higher than the load that the cylinder experiences, lower displacement for a higher load can be observed. In a drop-hammer test, the position of the load cell is between the hammer and the cylinder, so it measures the resistance of the cylinder and the resistance of the inertial force, or in other words, the external load. This information is consistent with the explanation of the strain-rate effect due to the inertial force, but the conclusion of an increase in the strength of the material means that the velocity of the mass is neglected; therefore, cannot be correct. Moreover, the velocity at failure can be seen in videos taken during Krauthammer and Elfahal's (2002) tests when fragments of mass burst out with velocity at failure.

For this study, a two-part split cylinder from Krauthammer and Elfahal (2002), as can be seen in Fig. 3-1 (a), will be examined. The problem will be divided into two parts, pre-failure and post-failure. The first is before the concrete reaches ε_{cr}, a tensile strain that fails the concrete. For a specimen subjected to a compressive load in the vertical direction, y, in the pre-failure stage, the compressive stress in the load direction causes

a compression stress in the vertical direction and a tensile strain in the horizontal direction corresponding to Poisson ratio

$$\varepsilon_y = -\frac{\sigma_y}{E} \tag{3-1}$$

$$\varepsilon_x = -\frac{\nu\sigma_y}{E} \tag{3-2}$$

where ε_y and ε_x are the strain in the vertical and the horizontal direction respectively, σ_y is the compressive stress in the load direction, E is the module of elasticity, and ν is the Poisson ratio.

In a cylinder, unlike the mass-spring system, the action of an applied force is not transmitted at once to all parts of the body, and deformations produced by the force are propagated through the body in the form of waves. In a dynamic domain in high load rates, if the dimensions of the body are large, the time taken by the waves to traverse the body becomes important. They presented the following two velocity equations

$$c = \sqrt{\frac{E}{\rho}} \tag{3-3}$$

$$v = \frac{\sigma}{\sqrt{E\rho}} \tag{3-4}$$

where c and v are the stress propagation wave velocity through the material and the velocity given to the particles in the affected zone by the stress wave, respectively.

In the post-failure stage, the specimen is separated into macro-fragments of mass, each with a direction and velocity. Some examples can be seen in Fig. 3-1 (a), (b), and (c). As said before, the specimen in Fig. 3-1 (a) will be examined. In that case, the specimen is divided into two rigid parts with motion in the horizontal direction and with a remaining velocity from the pre-failure stage. The post failure stage will be discussed in

more detail later in the post-failure stage section. The cylinder will be examined by using a finite element method, which will be explained in the finite element analysis section.

Poisson Failure in a Mass-Spring System

In order to understand the mechanism of a Poisson characteristic of failure, a mass-spring system with a lumped mass, M, and a linear spring of stiffness, K, as can be seen in Fig. 3-2, will be examined first. The point of interest in the mass spring system is not the direction of the load but the horizontal direction that Poisson effect is sound because the crack opens due to the strains in this direction. In the dynamic domain, inertial forces correspond to the movement of the mass are involved. For the mass-spring system, as in the cylinder, the Poisson failure occurs when the displacement of the spring reaches a maximum value, x_{cr}. Chandra and Krauthammer (1995) suggested that the influence of the inertial force in the dynamic domain explains the strain-rate effect, as shown in Chapter 2. Their study showed that the inertial force causes a difference between what the external load applies, P(t), and the actual load that acts on the spring, Fs(t). The displacement of the spring corresponds to Fs(t). So when P(t) is higher than Fs(t), lower displacement for a higher load can be observed. In conclusion, in the dynamic domain, a specimen can be subjected to higher loads than the static nominal failure load without fail. This study adopts the explanation above, in which the inertial force is the main cause to observe strain-rate effect, but suggests a reexamination of the conclusion. Inertial force appears when the mass has non-zero velocity. This velocity means that the displacement of the spring continues to increase even after the external load is no longer applied. If at failure the mass had had a velocity, the specimen would have been failed due to a lower load than the applied load. The nominal failure load in the dynamic domain is not the load at failure but the load

that causes a zero velocity of the mass at failure. The sum of the displacement due to the load and the displacement due to the velocity of the mass should be equal to the critical displacement, X_{cr}. A solution can be easily obtained by using the equations of motion. The displacement due to the load is obtained by the forced-vibration stage, and the displacement due to the velocity of the mass when the load stops is obtained by the free-vibration stage. In the results chapter, several examples are examined for validation.

Conclusion of Inquiry on the Strain-Rate Effect

There are two principle differences between the static domain and the dynamic domain. First, in the dynamic domain there is a difference between what the external load applies and the actual load that acts on the spring due to the appearance of the inertial force. The second difference is that in the dynamic domain the appearance of the inertial force causes the mass to have a non-zero velocity at each point of time. As explained in the last two sections, the first difference is the reason for the observation of the strain-rate effect. It explains the strengthening observed in the stress-strain curve in various load rates, and it explains the strengthening observed in the nominal strength at failure in various load rates. The influence of the second difference on the strain-rate effect has not been examined in previous studies. This study examines the assumption that if the second difference is taken into account, then the specimen's strength will not change in various load rates as expected according to the current method, and the strain-rate effect might be a result of an incorrect conclusion. The strengthening observed in the nominal strength at failure is incorrect, because the failure load is not the load at failure, which leaves the mass with a non-zero velocity, but is the load that causes a zero velocity of the mass at failure. The assumption of this study is significant:

it implies that the nominal strength at failure of a specimen in the dynamic domain is lower than the strength measured with the drop hammer test. If this method is approached with split Hopkinson test, the results should be checked once again, and the Dynamic Increase Factors (DIF), which can be found in the Euro code (CEB, 1993), are questionable. The following sections suggest a technique based on an energy method for examining a failure in the dynamic domain.

Basic Concepts of the Suggested Method

The strain energy release rate for crack propagation (Surenda, Stuart, & Ouyang, 1995), introduced in Chapter 2, suggests that the total potential energy is equal to the work done by applied force, the strain energy of the structure, and the energy for crack formation, as can be seen in Eq. 3-5 In the dynamic case, an additional kinetic energy is applied, as follows:

$$\Pi = U - F + W + Ek \tag{3-5}$$

where Π is the total potential energy, F is the work done by applied force, W is the energy for crack formation, and U and Ek are the strain and the kinetic energy of the structure, respectively.

Eq. 3-5 presents the whole process during the formation and propagation of a crack. This study proposes that the crack formation process be divided it into two stages: the pre-failure stage, which is defined as just before the appearance of the crack, and the post-failure stage, which is defined as just after the occurrence of a failure when a crack propagates through the entire cylinder, without examining the propagation stage. In the first stage the energy equilibrium is equal to:

$$\mathrm{F} = U + Ek \tag{3-6}$$

Let Ecr be the strain energy corresponding to the cracking tensile strain of the specimen. If U is less than Ecr, part of the kinetic energy will transform into strain energy until the appearance of a crack, and Eq. 3-6 can be written as

$$\mathrm{F} = Ecr + \Delta Ek \tag{3-7}$$

where ΔEk is the remaining energy after the formation of the crack.
Note that the remaining energy is not necessary for the pre-failure stage because the tensile strain in the cylinder is already equal to the cracking tensile strain and this extra energy continues to the post-failure stage.

Let Eex be the extra energy which continues into the post-failure stage, as follows:

$$Eex = \Delta Ek = F - Ecr \tag{3-8}$$

In the post-failure stage, the most significant energies are the energy for crack formation, which is the surface energy of the surfaces of failure, Esu, and the kinetic energy of the fragments, Ek.

$$Eex = Esu + Ek \tag{3-9}$$

This study proposes that the extra energy is responsible for the character of the failure.

Energy Method

An approach based on energies equilibrium might be the most comprehensive way to analyze the failure. For the same spring-mass system, which was described in Fig 3-2, an external quasi-static loading of the system means that the load is subjected

gradually to the system at the same loading rate as the rate of the resisting capability of the system to an applied load. The work done by an external load is equal to

$$W = \int_0^x F(x)dx \tag{3-10}$$

where F(x) is the external load, and X is displacement of the mass.

The strain-energy is equal to

$$Es = 0.5KX^2 \tag{3-11}$$

where K is the stiffness of the spring.

In the quasi-static domain, the strain energy is the only energy developed in the system, so all the work done by the external load is equal to the strain energy, as follows

$$W = Es \tag{3-12}$$

Any loading rate above the resisting-capability rate of the system will result in a velocity of the mass in addition to the displacement, so the work done by the external load is equal in this case to the sum of the strain energy and the kinetic energy

$$W = Es + Ek \tag{3-13}$$

$$Ek = 0.5MV^2 \tag{3-14}$$

where V is the velocity of the mass.

In high loading rates, the kinetic energy becomes much more significant than in low loading rates. As a result, for the same work done, the strain energy obtained is

lower in high loading rates than in low loading rates, as can be seen in the following equation

$$Es = W - Ek \tag{3-15}$$

The observation above is consistent with the rate-effect phenomenon, which points to an increase of the nominal strength at failure in high loading rates. In other words, the same value of maximum stress will result in strain that is lower in high loading rates than in low loading rates, and so the nominal strength at failure will be increased.

As in the previous section, the above explanation does not represent the whole picture. It is true that the specimen exhibits lower strain, but, in contrast to the static loading, it also has velocity. This velocity will cause the mass to continue with the movement until the velocity reaches zero, even after the external load has been stopped, and so the strain of the specimen will continue to increase. In other words, due to the law of conservation of energy, the strain energy will increase as the kinetic energy decreases without interference of an additional external load. This might imply again that the rate-effect phenomenon is insubstantial, and that the increase in the nominal strength at failure under high loading rates does not point to a strengthening of the material. If the mass has enough time to move, then the specimen will fail under lower strength than the above.

Energy Method With Respect to a Time-Line

A time-line seems to be a very important factor when the effect of high loading rates is examined. Two factors might be varied with respect to time and should be followed: the applied load and the displacement of the mass. In order to use the energy

method, a relation between the applied load and work done by the applied load with respect to time needs to be found. This relationship can be obtained in two steps: the displacement of the mass with respect to time as a result of an applied load varied in time can be found from an equation of motion, and then the work done can be calculated as follows

$$W = \int_0^t U(t)F(t)dt \tag{3-16}$$

Where U(t) is the displacement of the mass, F(t) is the applied load, and t is the duration of the load.

Failure Criterion Based on Energy Method

Based on the above information, when one wants to know whether the system fails under an applied load, the following procedure should be carried out: the displacement as a function of time, U(t), can be calculated from the equation of motion then the work done, W, can be calculated from Eq. 3-16. The crack appears when the displacement in the spring is equal to the ultimate displacement of the spring, U=Uult, and the critical amount of energy that fails the system is equal to

$$Ecr = 0.5KUult^2 \tag{3-17}$$

where K is the stiffness of the spring.

The failure occurs when

$$W > Ecr \tag{3-18}$$

The failure criterion based on the energy method, as represented in Eq. 3-18, is an independent strain-rate effect criterion. In high loading rates the kinetic energy at the beginning of the movement is much higher than in low loading rates, a difference which

is significant to a failure criterion based on the influence of the inertial force, as represented in section 2.8. Because of the conservation of energy consideration, even if the strain energy is not high enough to cause fail at the beginning of the impact, the kinetic energy will eventually transfer to strain energy until a failure occurs, when U = Uult. So to determine whether the failure occurs, the only question should be: is the work done by the applied load more or less than the critical energy of the system? Note, that for failure to occur in a cylinder, the crack must propagate through all the surface of failure and the critical energy is therefore more complicated to obtained, as will be explained in the post-failure stage section.

P-I Curve

An impulse load is an interesting problem to examine. During an impulse load a specimen can be subjected to an extreme-high load for an extreme-short duration of time that produces a small amount of work. According to the new criterion of failure, in some cases the specimen will not fail even though the load is higher than the static capacity load of the specimen because the total amount of energy is below the critical energy. It seems to be that P-I curve (Krauthammer, Modern protective structures, 2008) is the correct way of presenting if failure occurs or not in the dynamic domain. A P-I curve is a Pressure-Impulse diagram. The impact load can be defined in terms of peak load and impulse load, which are defined in terms of pressure/force and duration respectively. The impulse is defined as the area under the load-time curve as can be seen in Fig. 3-3. Impulsive asymptote represents the strain energy equals to the kinetic energy because the highest theoretical load rate is applied while quasi-static asymptote represents work equals to the strain energy as there is no kinetic energy applied into the system (static loading.) Using the procedure from the section above, the nominal

strength at failure can be found for various values of impulse, and a P-I curve can be developed. In the result chapter, this study will generate a P-I curve by using the new criterion of failure.

Post-Failure Stage

The next stage is to examine what happens after the failure occurs. At that point, there is an amount of extra energy that can be calculated as

$$Eex = W - Ecr \tag{3-19}$$

This study proposes that the extra energy is responsible for the character of the failure. The simplest case is when the extra energy is equal to the minimum amount of energy for crack formation, a case in which the character of the failure is only the appearance of a crack. In more complicated cases, when the extra energy is higher than zero, the extra energy can cause additional surfaces of failure or fragments of mass with velocity or both. A fracture mechanics approach based on energies equilibrium can be a way to obtain the amount of energy that is needed for each character of failure. The strain energy release rate for crack propagation (Surenda, Stuart, & Ouyang, 1995), introduced in chapter 2, suggests that the total potential energy is equal to the work done by applied force, the strain energy of the structure, and the energy for crack formation. In this dynamic case additional kinetic energy is applied. As mentioned before, a two-part split cylinder from Krauthammer and Elfahal (2002), as can be seen in Fig. 3-1 (a), is examined. The minimum amount of energy needed for this case is equal to the energy for crack formation in a size of the surface of failure. The amount of the extra energy will be equal to the difference between the external work and the critical energy. The kinetic energy of the remaining velocity of the mass is

part of the extra energy. A finite element model will be used to calculate the critical energy, as will be explained in the following section.

Finite Element Analysis

For a cylinder analysis, the mass-spring system cannot be used in order to analyze what happens inside the mass since the mass is distributed and not concentrated; therefore, the problem will be analyzed utilizing a finite element model. A model of a 24 (in) x48 (in) cylinder made of concrete will be analyzed in ABAQUS explicit version 6.10. The analysis is performed in two stages. First, the impact will be obtained by a theoretical concentrated triangular load on the top of the cylinder, which will be defined as a rigid body. The purpose of this analysis is to examine principles of the behavior of a multi-degree of freedom system in a dynamic domain. Second, the actual stress that was captured by the load cells from Krauthammer and Elfahal's (2002) tests will be subjected as a distributed stress on the top of the cylinder. The purpose of this analysis is to examine the differences that might be when using a drop-hammer test and to try to explain the results.

Summary

The goal of this study is to explain one of the several modes of failure that occur by utilizing Krauthammer & Efahal test and try to understand the rate observed in this test. In order to reach this goal the following methodology was observed: two basic assumptions were made first being that the inertial force is the most significant cause of rate effect and the second being concrete fails due to tensile strain. The mechanism that controls the failure in the mode that is analyzed is the Poisson effect. To understand the influence of inertial forces on the dynamic domain, the mass spring system was analyzed first. Criterion of failure based energy method was implemented to

represent the failure in the dynamic domain, and finally the cylinder was examined utilizing finite element model.

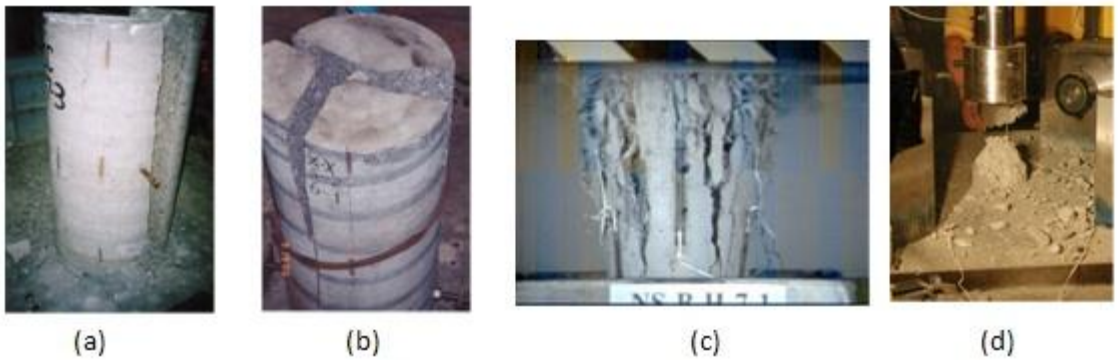

Figure 3-1. Poisson characteristic of failure (Krauthammer & Elfhahal, 2002)

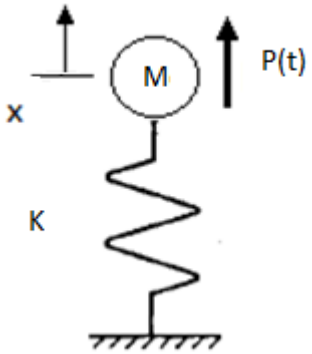

Figure 3-2. A mass-spring system

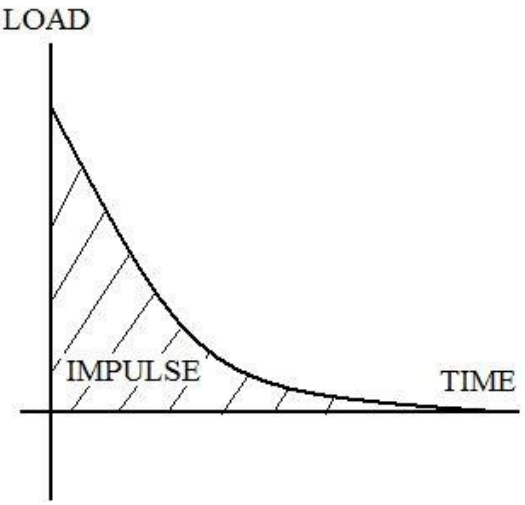

Figure 3-3. A definition of an Impulse

CHAPTER 4
RESULTS

A Mass-Spring System Analysis

The failure occurs in the lateral direction of the cylinder while the compression is in the longitudinal direction, which is explained by the Poisson effect. Analogy of the mass spring system clarifies the mechanical deformation on the cylinder in the lateral direction.

Chandra and Krauthammer (1995) showed that the inertial force causes a difference between what the external load applies, P(t), and the actual load that acts on the spring, Fs(t) , as shown in Chapter 2. In this section the influence of the velocity of the mass on the failure load and the suggested failure criterion will be examined. A lumped mass, M, and a linear spring of stiffness, K, as can be seen in Fig. 4-1(a), is subjected to a dynamic force, P(t), as can be seen in Fig. 4-1(b), varying with time, t, given by

$$P(t) = \alpha t \tag{4-1}$$

where α is the loading rate.

Example features were chosen for representing the problem. The features of the mass-spring system are presented in Table 4-1. For these features, the critical energy is equal to

$$Ecr = 0.5KXcr^2 = 2.5e6\ (N \times mm) \tag{4-2}$$

and the nominal strength at failure, for the static domain, is equal to

$$Fst = KXcr = 5e6\ (N) \tag{4-3}$$

The governing equation of motion for the forced-vibration motion, $t < \tau$, is presented in Chapter 2.

The governing equation of motion for the free-vibration motion, $t > \tau$, is

$$M\ddot{x} + Kx = 0 \tag{4-4}$$

and the solution is

$$x(t) = X_\tau \cos\omega(t-\tau) + \frac{V_\tau}{\omega}\sin\omega(t-\tau) \tag{4-5}$$

$$X_\tau = \frac{\alpha}{K}(\tau - \frac{\sin\omega\tau}{\omega}) \tag{4-6}$$

$$V_\tau = \frac{\alpha}{K}(1-\cos\omega\tau) \tag{4-7}$$

In the first case when the work done is higher than the critical energy of the system, the applied load, P(t), and the internal force in the spring, Fs(t), are shown in Fig. 4-2(a), which represents examples of two various load rates. The displacement in the spring during the duration of the applied load is shown in Fig. 4-2(b). The displacement in the free vibration stage is shown in Fig. 4-2(c). In Fig. 4-3 and Fig. 4-4, the same plots as in Fig. 4-2 is shown, but only for a case when the work done is equal and lower that the critical energy of the system, respectively. In the second case that amount of work reaches the value of critical energy, as seen in figure 4-3, when the load is applied, the displacement of the spring does not reach the ultimate crack length, x_cr; however, this does not indicate that the spring will not fail since the displacement continues and reaches the x_cr during the free vibration motion. In the final case where the critical energy is greater than the amount of work, as seen in figure 4-4, the failure will not occur, even during the free vibration motion. In Table 4-2, a summary of the

results from the three cases can be found. The results obtained using MathCAD code, which can be found in Appendix A.

P-I Curve for a Mass-Spring System

As can be seen in the results above, the amount of external work and the critical energy of the system will determine if a failure occurs. Based on the results, a P-I curve is an efficient way to present the criterion of failure in the dynamic domain. Using the equations of motion, the nominal strength at failure can be found for various values of impulse, and a P-I curve can be developed as the following: for a given load function, the displacement as a function of time, U(t), can be calculated from the equation of motion such that the work done is equal to the integral over time on the product of the applied force and the resulted displacement. The crack appears when the displacement in the spring is equal to the ultimate displacement of the spring, where $U=U_{ult}$; therefore, the critical amount of energy that fails the system can be defined as the strain energy when $U=U_{ult}$. Finally, the failure will occur when the amount of work is greater than the critical energy, E_{cr}.

As an example, a MathCAD code was developed to create a P-I curve for varied block-loads using the concept presented here. The P-I curve is shown in Fig. 4-5, where the axes are normalized: the load axis is normalized in a way that the static failure load is equal to 1and the impulse axis is normalized such that the highest impulse is equal to 1. Also, the MathCAD file can be found in Appendix B.

Summary of the Mass-Spring Analysis

Analysis of a mass-spring system subjected to a compression load with varied load rates and durations was made, and the following was observed:

1. The failure always occurred at the same internal force in the spring, although the external load at failure was changed among the cases.
2. When the load stopped, the mass continued to move in the same direction due to the velocity of the mass obtained during the duration of the load.
3. Although the relation of the kinetic and the strain energy were varied among the cases, the failure always occurred when the work done was equal to or greater than the cracking strain energy, which is defined as critical energy.
4. A P-I curve can be an efficient way to represent if a failure occurs according to the new criterion of failure.

Finite Element Analysis

For a cylinder analysis, the mass-spring system cannot be used in order to analyze what happens inside the mass since the mass is distributed and not concentrated; therefore, the problem will be analyzed utilizing a finite element model. A model of a 24 (in) x48 (in) cylinder made of concrete is analyzed in ABAQUS explicit version 6.10, as can be seen in Fig. 4-6. The analysis is performed in two stages. First, the impact is obtained by a theoretical concentrated triangular load on the top of the cylinder, which is defined as a rigid body. The principle shape of the load over time can be seen in Fig. 4-1(b). Second, the actual stress that was captured by the load cells from Krauthammer and Elfahal's (2002) tests is subjected as a distributed stress on the top of the cylinder. The results are taken from elements along the cylinder, as can be seen in Fig. 4-7. The observations from the two stages are presented in the following sections.

Theoretical Concentrated Triangular Load

The first observation is the time that takes the load wave to propagate. In multi-degrees of freedom systems, as the cylinder model, the load wave reaches each

element in a different time according to its distance from the subjected load and the material properties of the cylinder, as can be seen in Eq. 4-8 and Eq. 4-9.

$$c = \sqrt{\frac{E}{\rho}} \tag{4-8}$$

$$t = \frac{x}{c} \tag{4-9}$$

where c is the stress propagation wave velocity through the material, and E and ρ are the module of elasticity and the density of the material, respectively, x is the distance between the subjected load and the element, and t is the time that is taken the wave to reach the element.

When the material properties of the concrete cylinder (E=24800 MPa and ρ= 2.3E-9 tons/mm^3) are plugged in Eq. 4-8, the velocity is calculated as 3E6 (mm/s); therefore, the wave propagates from element 1 to 2 with 3E6 mm/s in 4E-4 seconds given the distance is equal to 200 millimeters when Eq. 4-9 is used (see Fig. 4-8.) The elements in this figure refer to the element numbers in Fig. 4-7.

It is important to take the time differences into account so the correct strain will compare to the stress applied. Moreover, when plotting a stress-strain curve for different load rates, if the time differences are not taken into account, a false rate-effect will be observed, as shown in Fig. 4-9 and Fig. 4-10. Although the load rate increases, the time of the wave propagation stays the same.

The second observation involves the energies distribution in the cylinder. The mechanism in multi-degrees of freedom system is different than in a mass-spring system. According to the theory of waves, an element, stores/releases energies depending on its location and the length of the stress wave. When the energies in the

whole cylinder are examined, the same concept of distribution of energies, as in the mass-spring system, is observed: during the time that the load applies, the kinetic and strain energy increase, then, when the load stops, the kinetic energy decreases and the strain energy increases, as can be seen in Fig. 4-11.

The last step is to calculate the amount of energy needed for the Poisson character of failure to appear. For a case when a cylinder is split into two halves due to the Poisson effect, the tensile strain of each element on the surface of failure must reach the cracking tensile strain of the concrete, ε_{cr}. According to the new criterion of failure, in order to determine if the failure can occur, the amount of external work should be higher than the critical energy of the cylinder. The critical energy can be defined as the strain energy needed for the first element located on the surface of failure to have a cracking tensile strain. Once the first element reaches a specific amount of ε_{cr}, each element on the surface of failure will reach that value in an order with the propagation of the wave.

A floor section was added to the FEM under the cylinder, as can be seen in Fig. 4-12, and a friction coefficient of 0.8 was defined between the surface of the floor and the bottom surface of the cylinder. The strength of the concrete used at the FEM is 4000 PSI (28 Mpa) and the corresponding cracking tensile strain is 0.00008 (Hsu, 1993). The static critical energy was calculated as 6.8E5 (N-mm) by using Eq. 3-17 and the time value was interpreted from Fig. 4-13 as 0.44E-3 (s); then taking this value and looking from Fig. 4-14 the strain value is read as 0.87E-5, which is extremely close to the theoretical value.

P-I Curve for a Cylinder

When the critical energy of the cylinder is known, a P-I curve can be generated to represent if a failure will occur in varied load rates. The time it takes for the work to reach the value of critical energy to cause failure is recorded for each load rate in Table 4-3. Then the peak load and the impulse values were calculated from the equations shown in the table. The resulted P-I curve is shown in Fig. 4-15. As can be seen, for a greater load the impulse needed for failure is lower.

Actual Test Load Model

Finally, an analysis of the actual test from Krauthammer and Elfahal's (2002) tests is performed. At that test, a Poisson characteristic of failure was observed, and the cylinder was split into two halves. It is hard to obtain the amount of external work applied, with the data that were documented, so the criterion of failure can be tested only in principle. A non-linear behavior was defined, using the Concrete Damaged Plasticity model, in the material properties of the concrete at the FEM. The cylinder was subjected to the same compression stress as the stress captured by the load-cells of that test. The load captured by the load-cells is shown in Fig. 4-16.

As in the theoretical study, the tensile strain of each element on the surface of failure must reach the cracking tensile strain of the concrete. The strength of the concrete used at the test was 4000 PSI. As before, the cracking tensile strain for that concrete is equal to 8E-5. The tensile strains of the elements located on the surface of failure are shown in Fig. 4-17, in which the element numbers refer to Fig. 4-7. The time of failure is the time that all the elements located on the surface of failure reaches the cracking tensile strain. The experimental data shows the time of failure is at 0.004 seconds (see Fig. 4-16), which directly correspond to the time of the cracking strain

occurring at element 7 (see Fig.4-18) as calculated by ABAQUS. On another note, the spikes seen in Fig 4-18 are due to the load waves travelling back and forth along the concrete cylinder during the impact.

The time value when the first element reached ε_{cr} was interpreted from Fig. 4-19 as 2.7E-3 (s); then taking this value and looking from Fig. 4-20 and Fig. 4-21 the critical strain energy value is read as 6.6E5 and the work value is read as 1.75E6, which is higher than the critical energy. When the actual test is examined, values fall in the higher range of the P-I curve, which indicates failure as experienced during the test (see Fig. 4-22.)

Summary of the Finite Element Analysis

Analysis of a cylinder subjected to a compression load with varied load rates and durations was made, and the following were observed:

1. The load wave reached each element at a different time according to its distance from the subjected load and the material properties of the cylinder. The time difference along the cylinder cannot be ignored, especially in high load rates.
2. In each element, the strain, stresses, and energies are determined by the duration of the load and by the location of the element in the cylinder. The movement of the load wave caused the distribution of the energies among the elements; therefore, the method used for the mass-spring system cannot be used in the same fashion on each one of the particles of the mass.
3. When tracking the energies of the whole cylinder, a similar behavior, as in the mass-spring system, was observed. After the load stopped, the strain energy increased due to the stocked kinetic energy in the system; however, in some cases the kinetic energy was not dropped all the way down to zero, which may have remained inside the concrete cylinder because of the dissipated energy by the wave propagation.
4. In the test analysis, according to the documentation of the loading history, the time it takes the split failure to occur matches the time of failure at the loading history.
5. In the test analysis, the critical energy of the cylinder was lower than the external work applied.

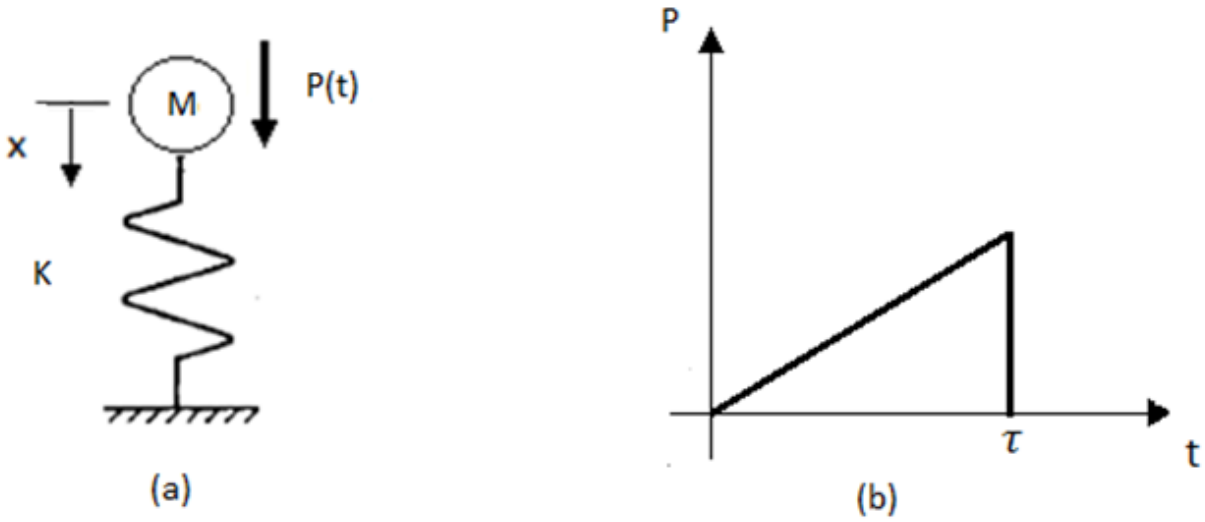

Figure 4-1. (a) A mass-spring system, (b) Applied load

Table 4-1. Input parameters used for the mass-spring system

M (t)	K (N/mm)	Xcr (mm)	A (N/sec)
0.5	5e6	1	10e10
			20e10

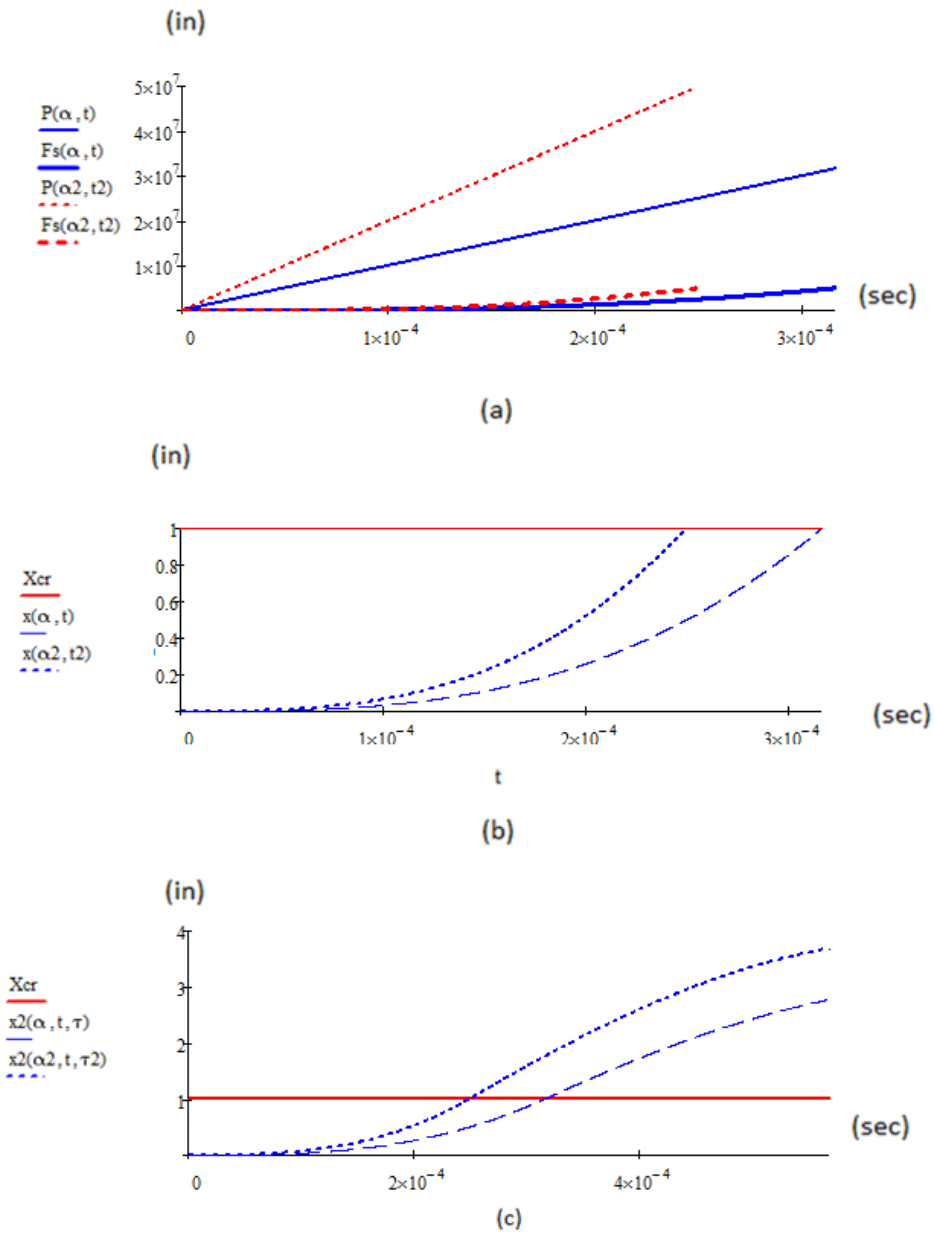

Figure 4-2. Case 1: W > Ecr

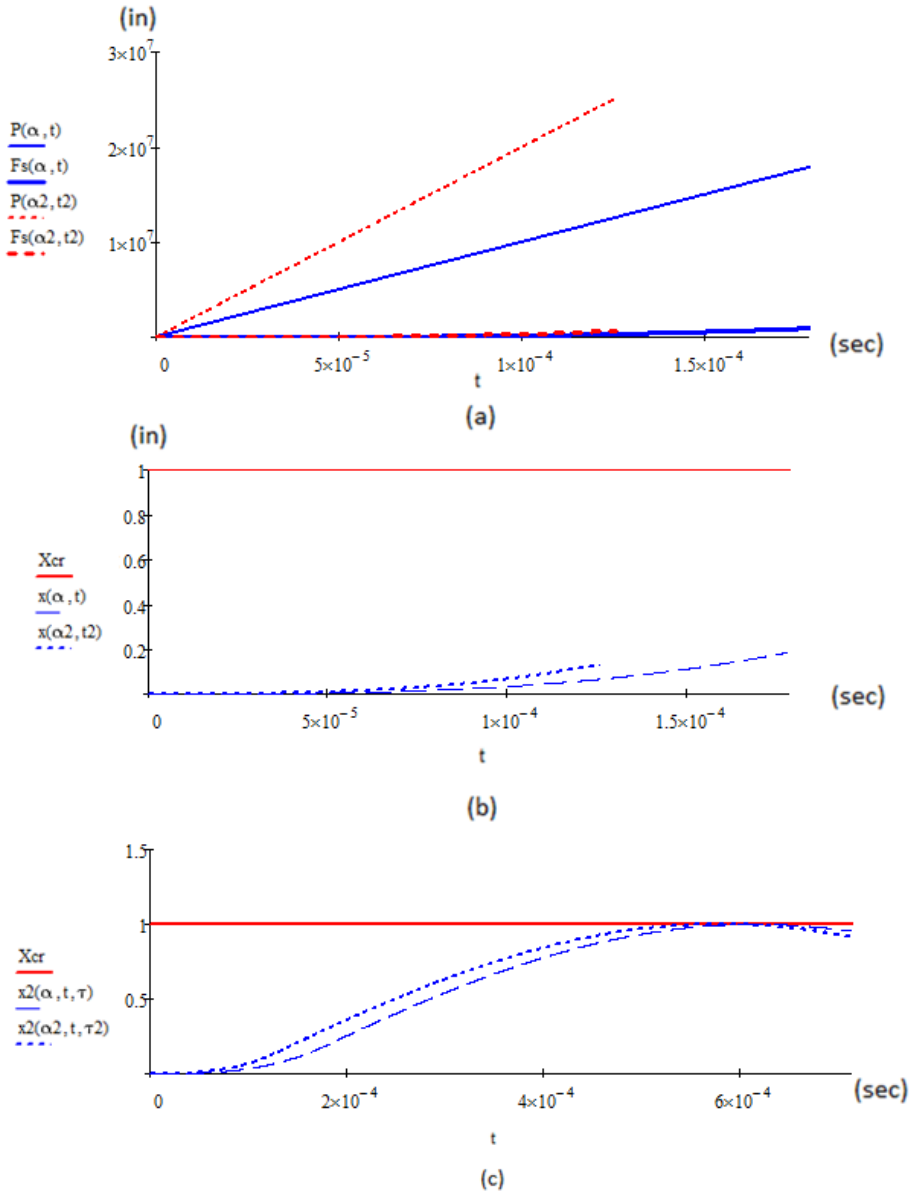

Figure 4-3. Case 1: W = Ecr

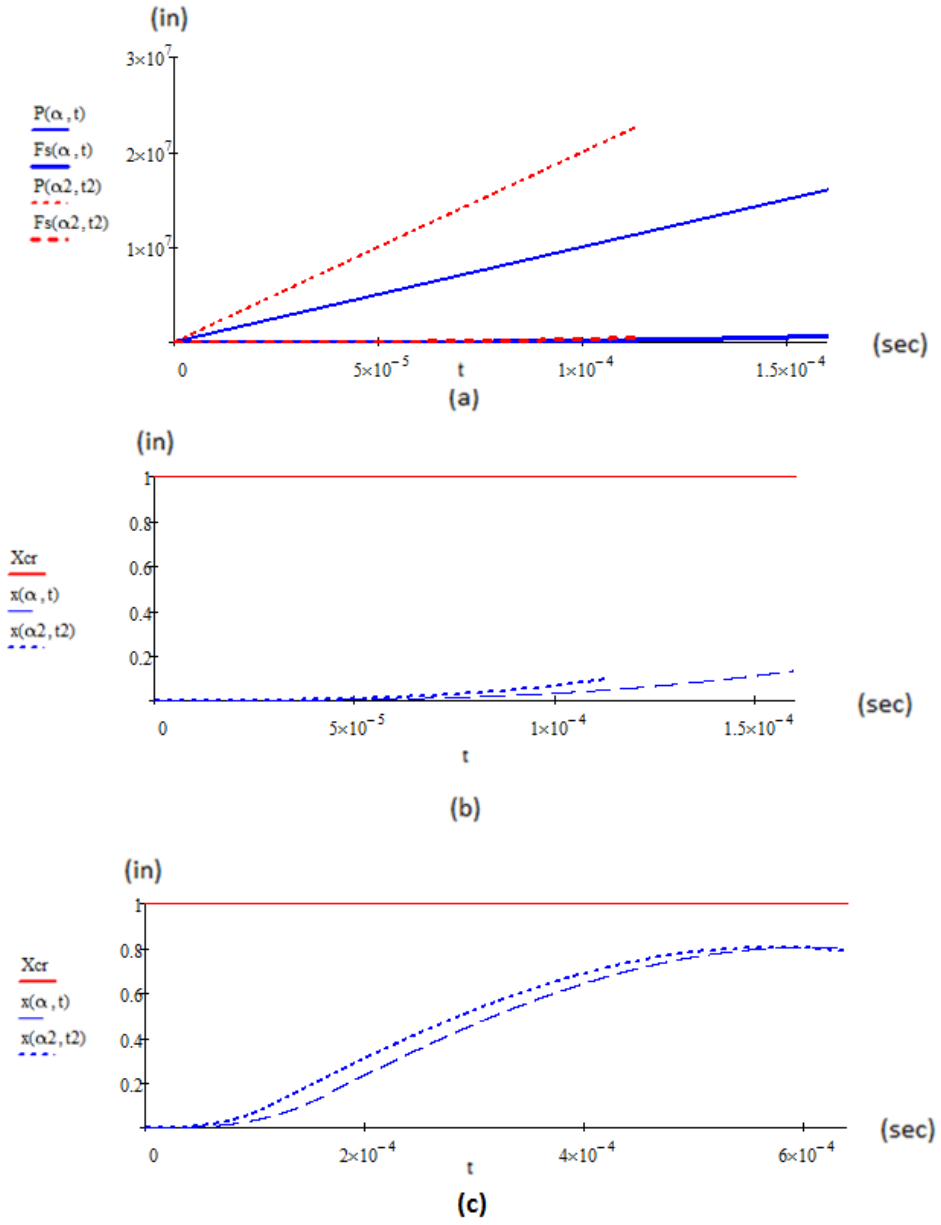

Figure 4-4. Case 1: W < Ecr

Table 4-2. Summary of MathCAD results

	A (N/sec)	P maximum (N)	Fs at failure (N)	Time at maximum P (sec)	Time at failure (sec)	Work done (N-mm)	Ecr (N-mm)
Case 1:	10e10	3.159e7	5e6	3.159e-4	3.159e-4	2.356e7	2.5e6
W>Ecr	20e10	4.984e7	5e6	2.492e-4	2.492e-4	3.725e7	2.5e6
Case 2:	10e10	1.786e7	5e6	1.786e-4	>1.786e-4	2.5e6	2.5e6
W=Ecr	20e10	2.52e7	5e6	1.26e-4	>1.26e-4	2.5e6	2.5e6
Case 3:	10e10	1.6e7	No failure	1.6e-4	No failure	1.615e6	2.5e6
W<Ecr	20e10	2.259e7	No failure	1.1293e-4	No failure	1.615e6	2.5e6

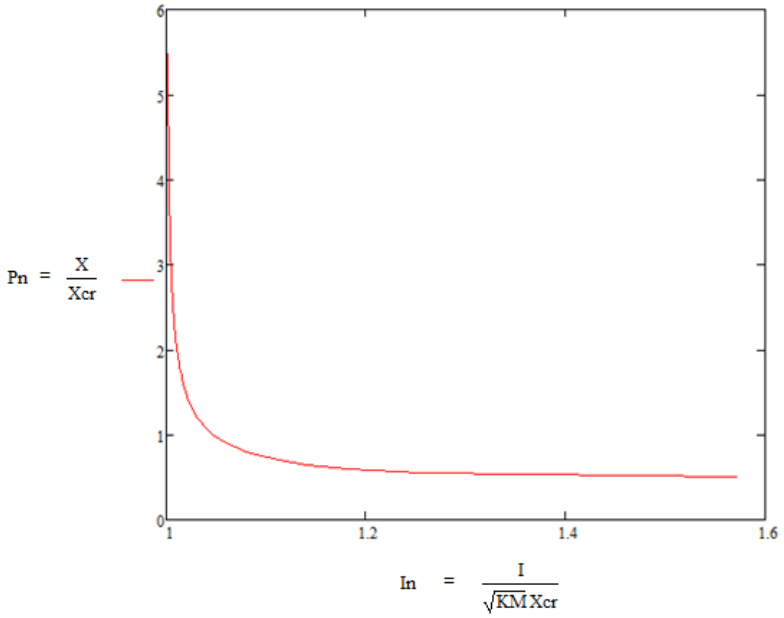

Figure 4-5. P-I curve

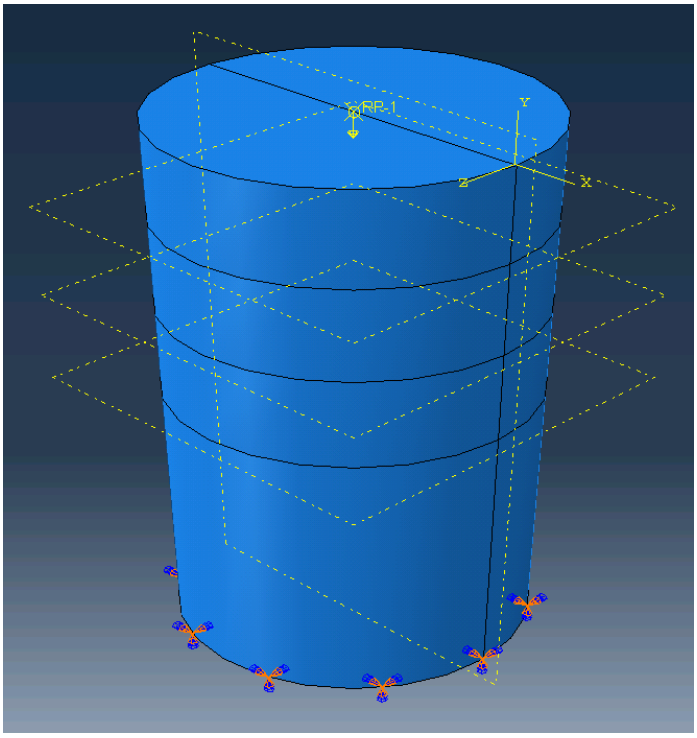

Figure 4-6. Cylinder model in ABAQUS

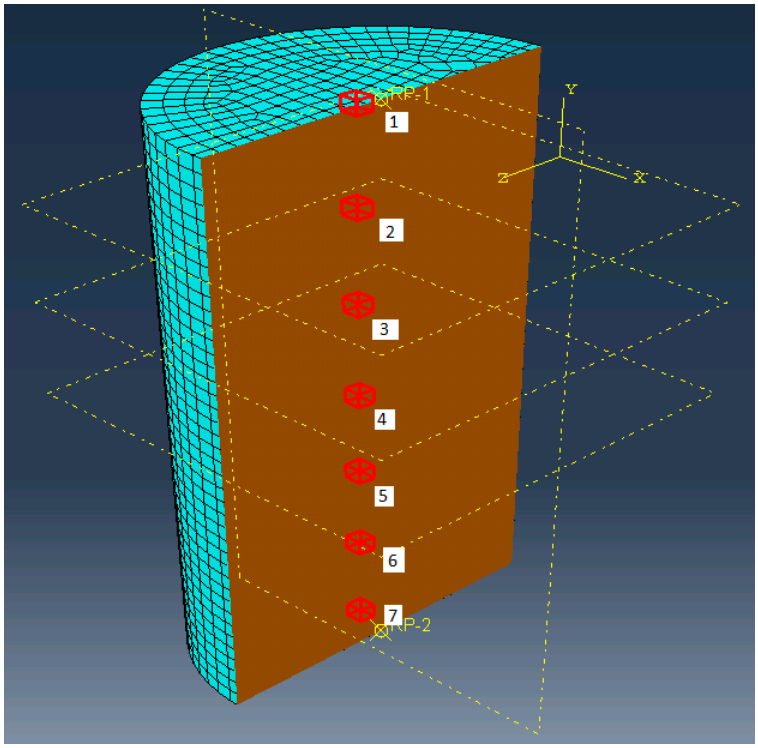

Figure 4-7. Elements examined along the cylinder

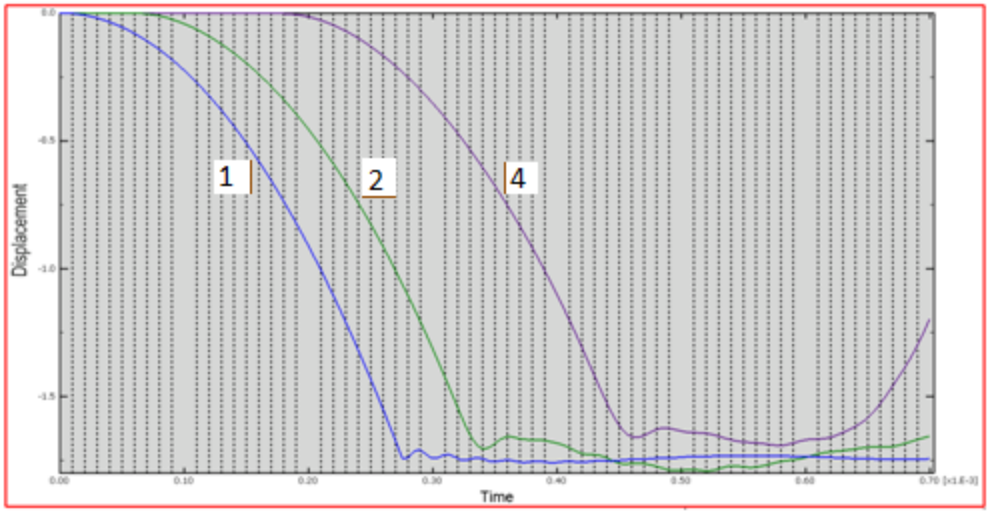

Figure 4-8. Elements examined along the cylinder

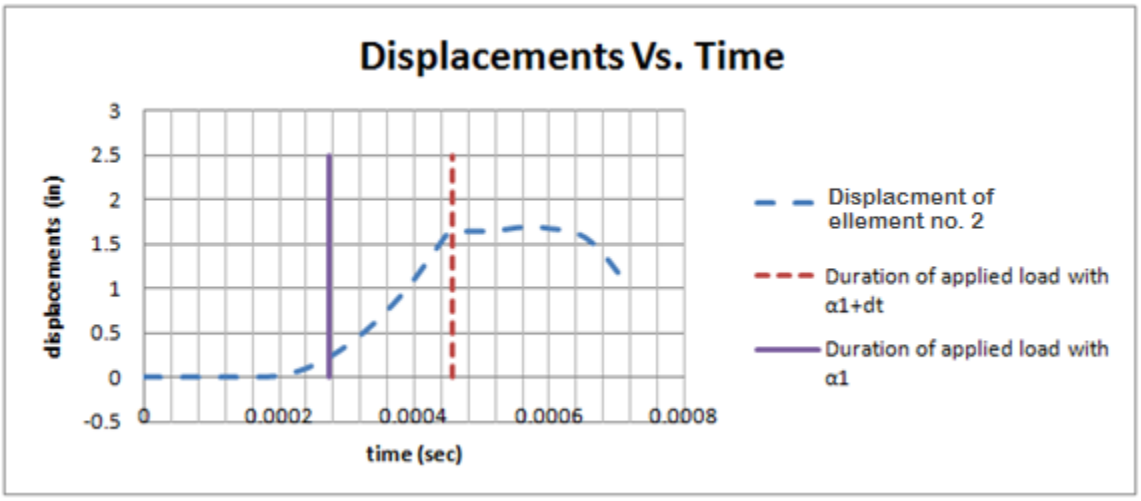

Figure 4-9. The influence of the time difference on the correct correspond strain

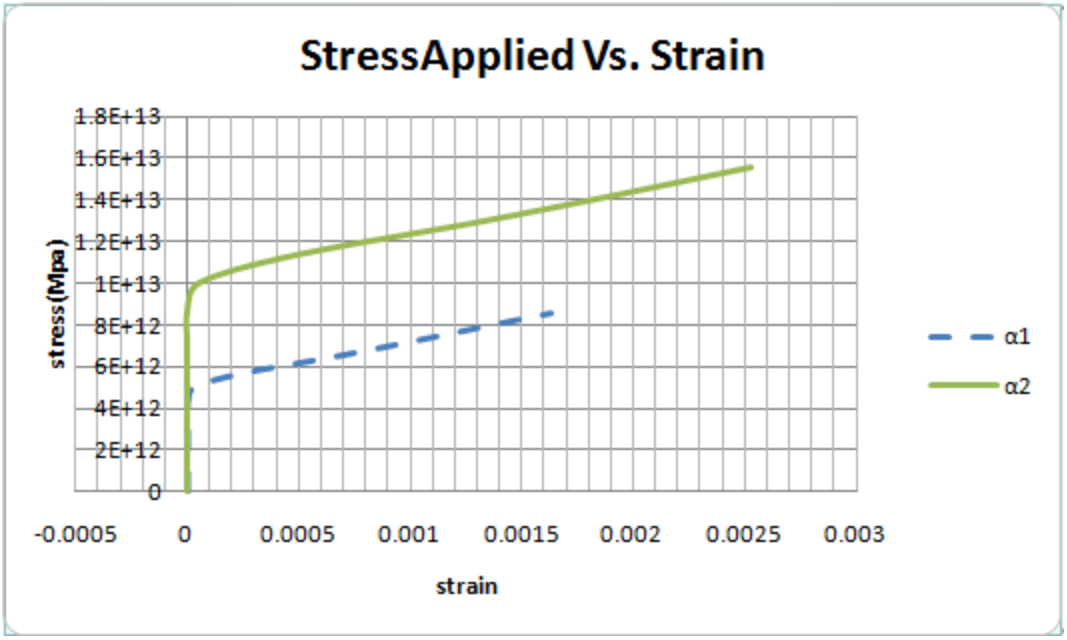

Figure 4-10. A false rate-effect observation

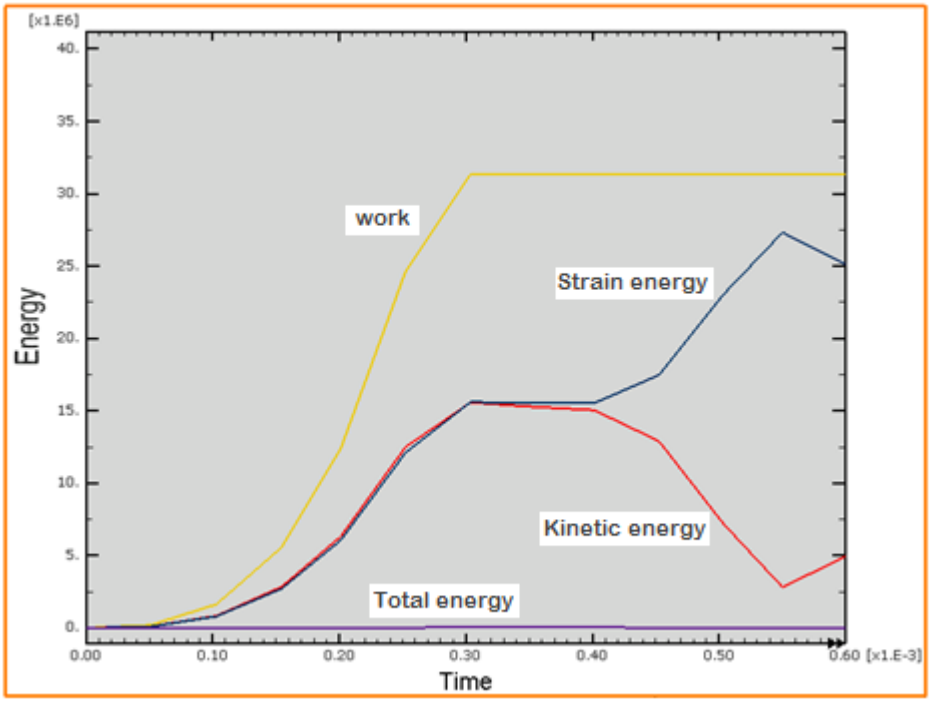

Figure 4-11. Energies distribution for the whole cylinder

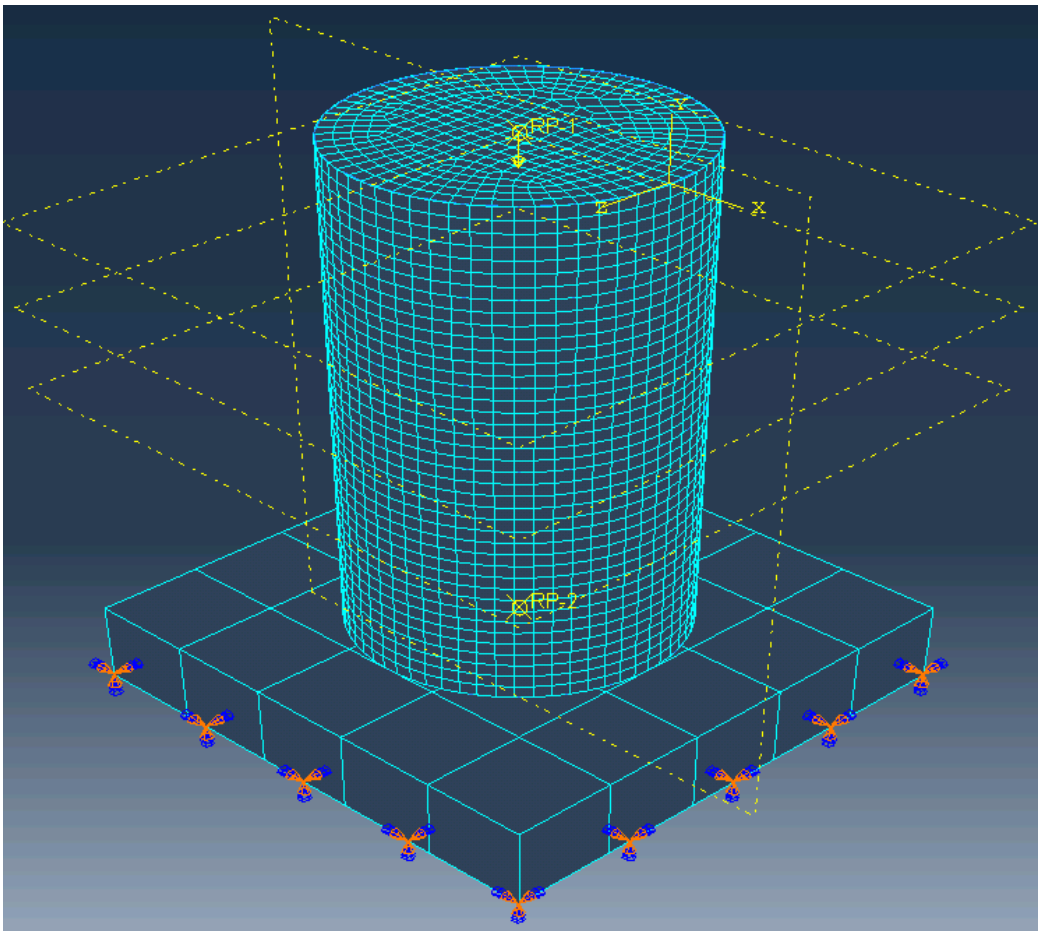

Figure 4-12. FEM of a cylinder and a floor

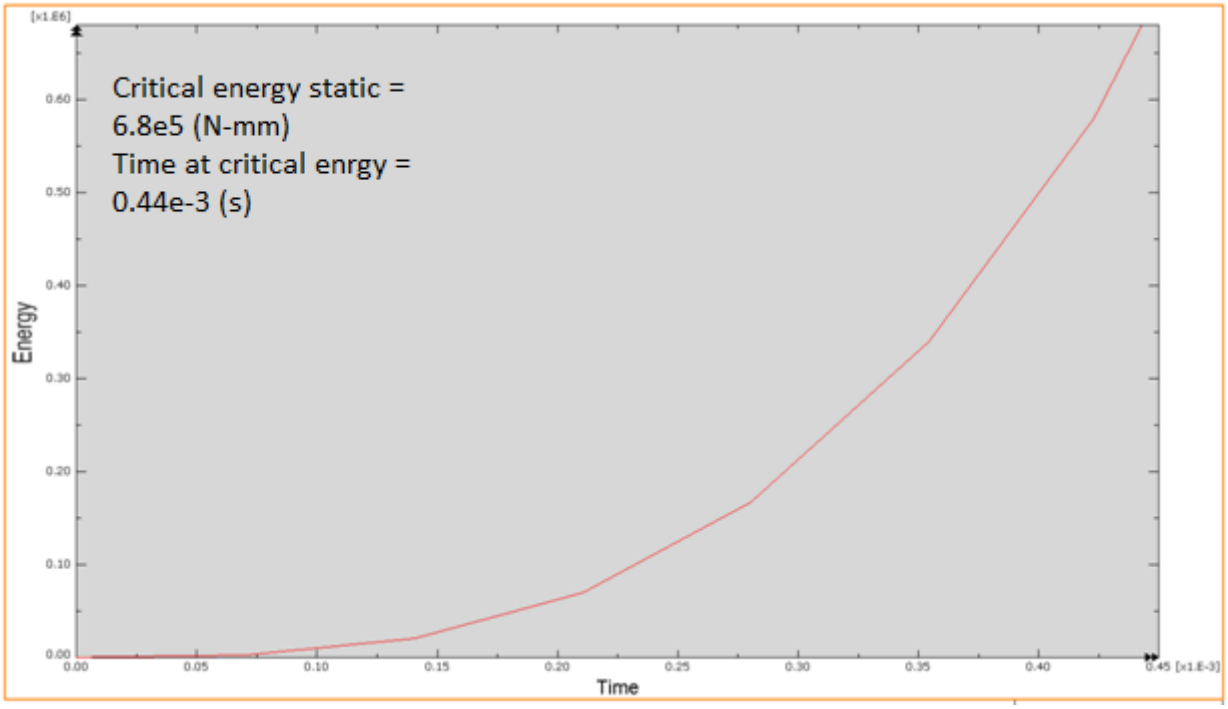

Figure 4-13. The strain energy of the cylinder

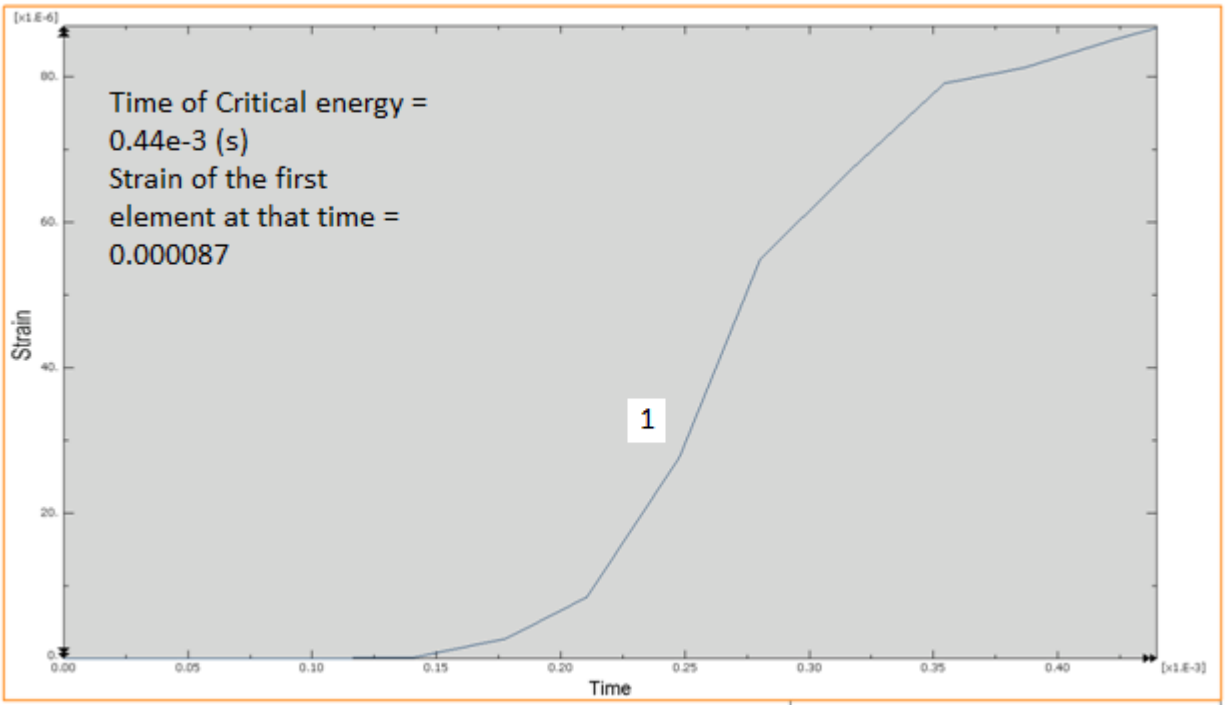

Figure 4-14. Strain of the first element

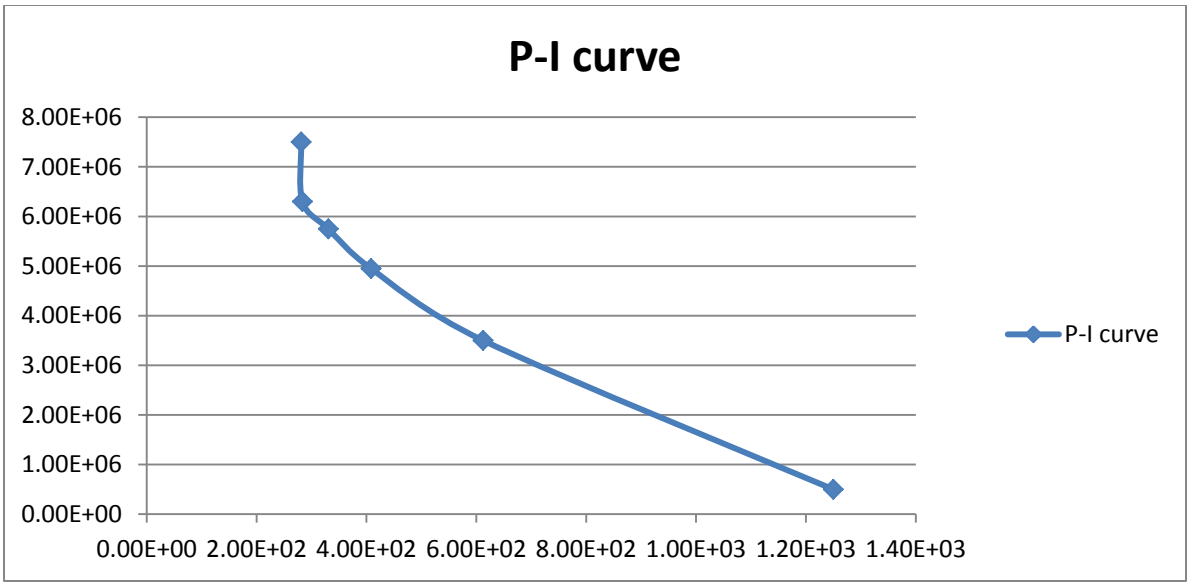

Figure 4-15. P-I curve

Table 4-3. Results of several load rates

Load rate(α) N/sec	t sec	P = αt N	I = Pt/2 N-sec
1E8	5E-3	5E5	1.25E3
1E10	3.5E-4	3.5E6	6.13E2
3E10	1.65E-4	4.95E6	4.08E2
5E10	1.15E-4	5.75E6	3.31E2
7E10	9E-5	6.3E6	2.84E2
10E10	7.5E-5	7.5E6	2.81E2

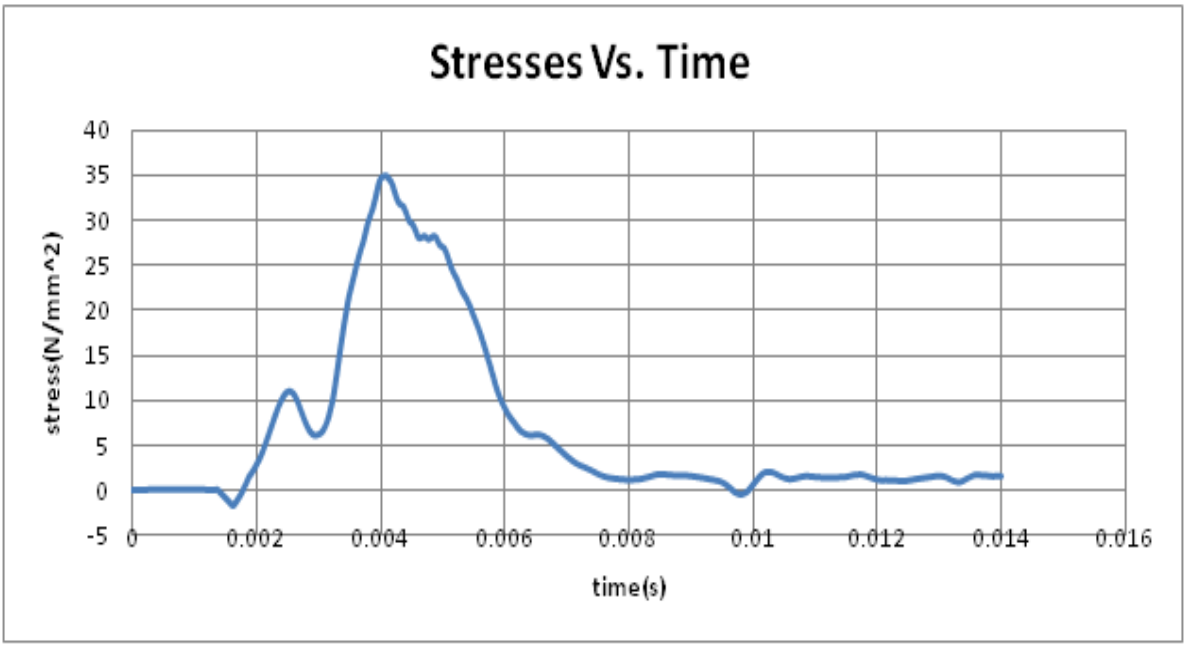

Figure 4-16. The load captured by the load-cells

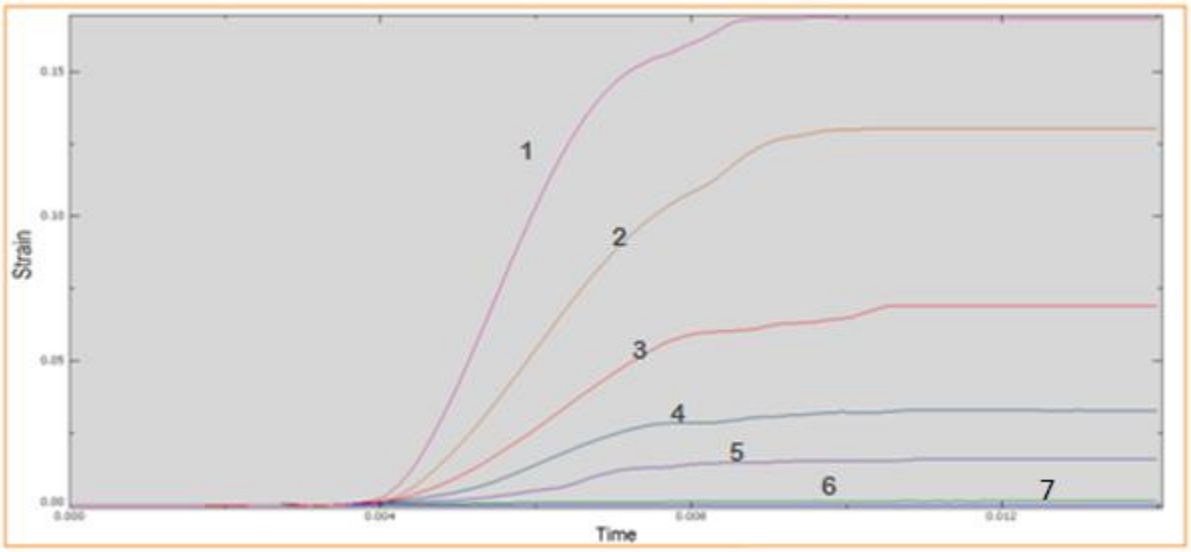

Figure 4-17. Tensile strain of elements located on the surface of failure

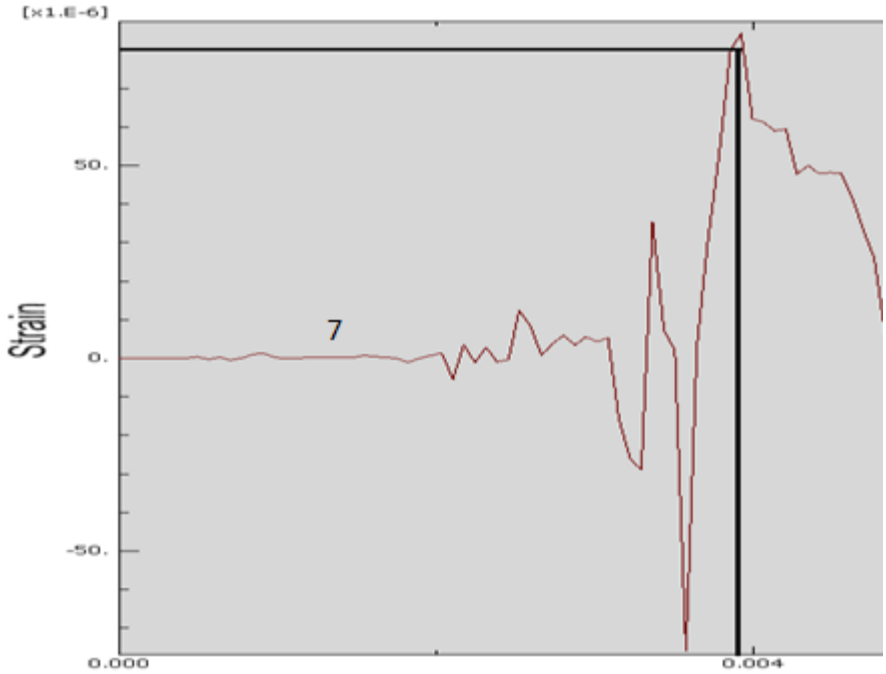

Figure 4-18. The time that took the last element to reach the cracking tensile strain

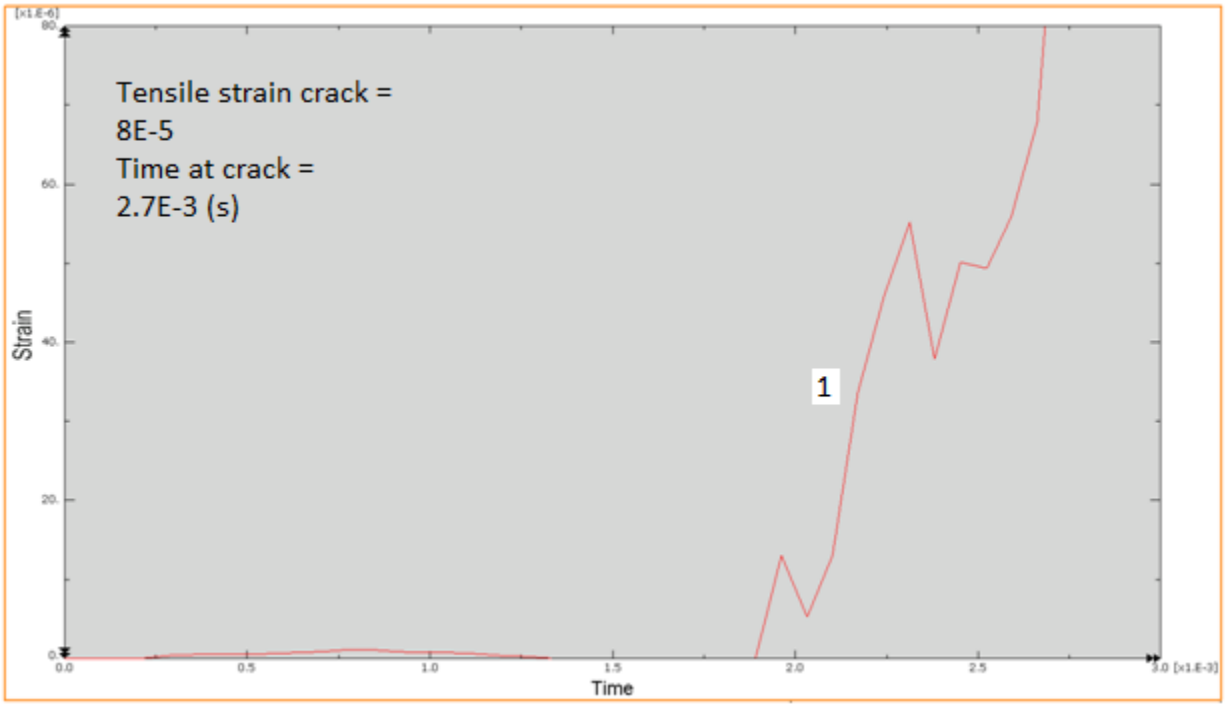

Figure 4-19. The time that took the first element to reach the cracking tensile strain

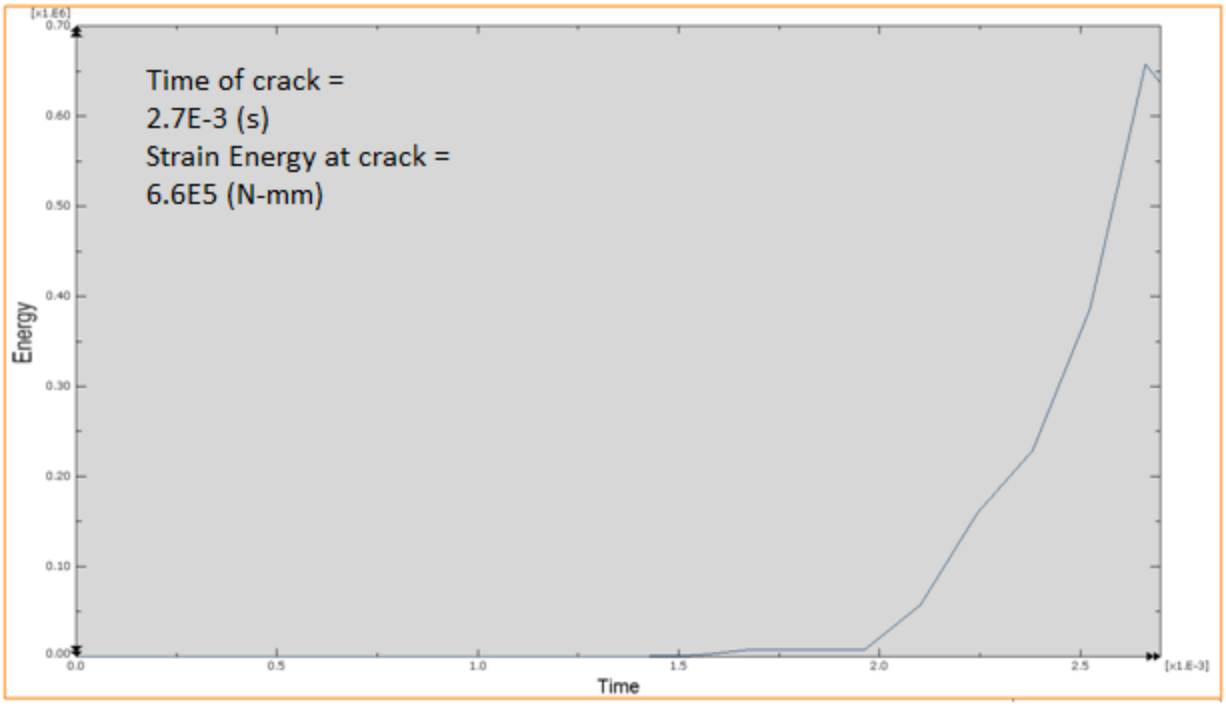

Figure 4-20. Strain energy of the cylinder

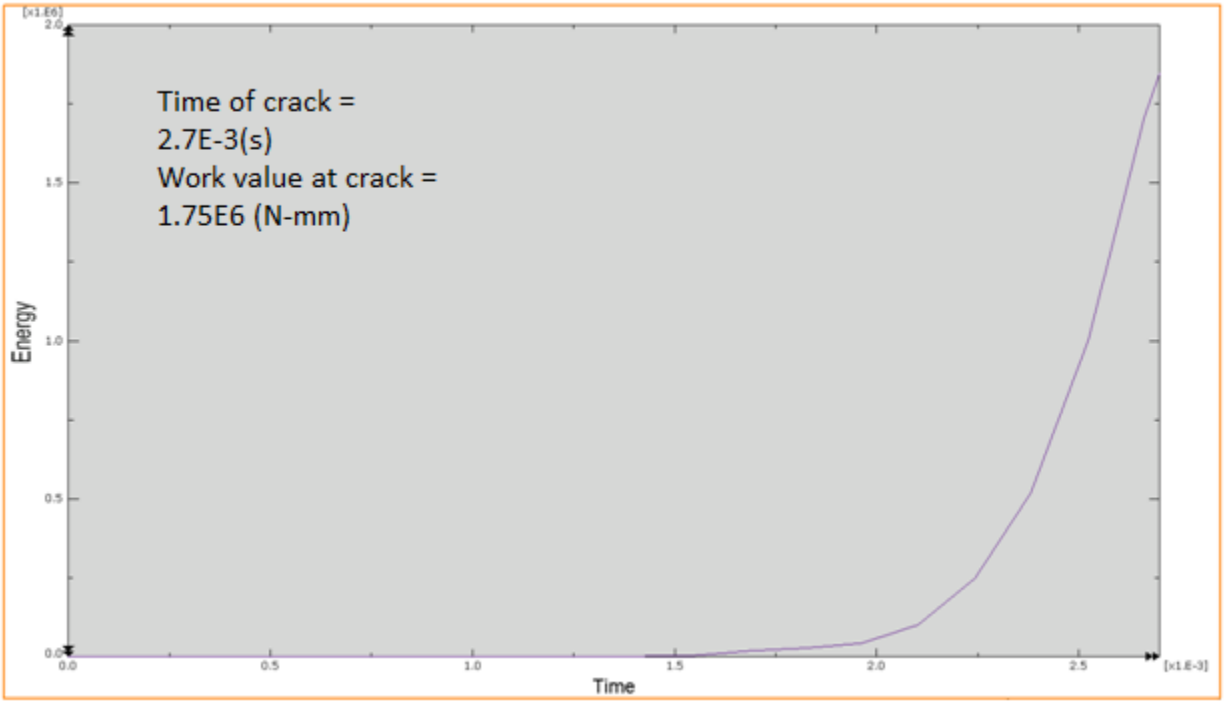

Figure 4-21. The amount of external work applied

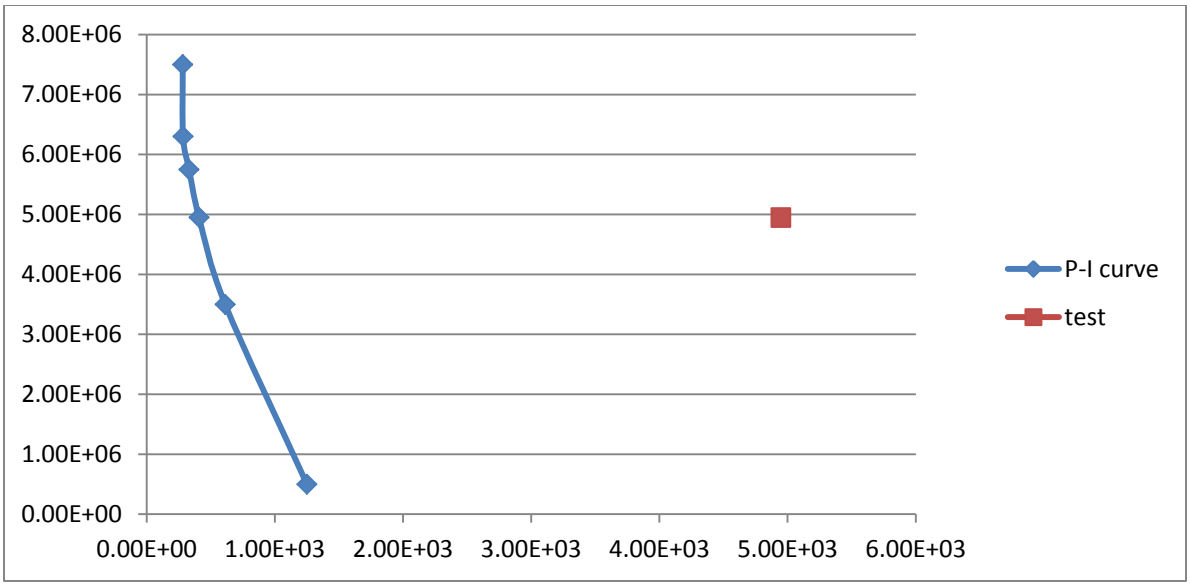

Figure 4-22. Actual test value on the P-I curve

CHAPTER 5
CONCLUSIONS AND RECOMMENDATIONS

Concluding Remarks

A new criterion of failure for a cylinder subjected to a compression dynamic load was examined with respect to the rate effect phenomenon, and two main analyses were completed. First, analysis of a mass-spring system using equations of motion method, and second, analysis of a cylinder uses finite element method. The following conclusions were obtained:

A. For the mass-spring system, the strengthening observed in the stress-strain curve is temporary. The correct strain that should be in that curve is not merely the strain that responds to the actual load that acts on the spring, but the summation of the last with the strain that responds to the velocity of the mass, which comes after a delay.

B. In the drop-hammer test, the load is obtained from a load-cell on the top of the cylinder, and the strain is obtained from strain-gauges along the cylinder. The time differences due to the load wave propagation must be taken into account, otherwise, a false rate effect will be observed in stress-strain curves for various load rates.

C. The load that caused the failure is not the load at failure. The load at failure leaves the mass with a non-zero velocity, or in other words, a potential increase of strain. The correct failure load is the load that causes a zero velocity of the mass at failure, which can be much lower. The strengthening observed in the nominal strength at failure during the drop hammer test should be reexamined.

D. For the mass-spring system, the suggested failure criterion predicted the failure correctly. For the cylinder, it was hard to implement the criterion, but still it predicted the failure in principle.

Recommendations for Future Research

The intent of the mass-spring system analysis was to study the principles of the mechanism of failure in a cylinder with respect to the rate-effect, and not to develop an analytical solution for the problem; however, it would be useful to have an analytical

solution instead of a numerical one. For this purpose, a multi-degree of freedom system should be analyzed, using the equation of motion or the theory of waves.

The results obtained in the finite element analysis cannot be validated in details due to the lack of additional observations needed from the drop-hammer test. The following procedure should be added to the test:

- The time difference of the load wave propagation between the load cell and the strain gauges should be taken into account.
- The rebound of the hammer after the impact, or the remaining velocity in the hammer before it stopped by the brakes, should be documented.
- It will be helpful to design a test of a cylinder subjected to a similar load rate but with a lower load from a different test of a cylinder that failed.
- The remaining velocity of the fragments at failure and their location at rest should be documented when possible.
- Strain-gauged in the Poisson direction can be helpful.

This study concentrated in analysis of the rate effect observed by drop-hammer tests. Another main method is the Split Hopkinson Pressure Bar test. Analysis of this method, as well as analytical and numerical solution will be another stage in understanding the failure mechanism under different load rates.

This study examined a Normal Strength Concrete. The same analysis can be done on a High Performance Concrete.

In the end, a person that jumps into the water from a very high height will die, even though the strengthening of the water is just temporary. It will be interesting to discover of ways in which the kinetic energy consumed is not strain energy, in order that the strengthening of the concrete will not be temporary.

APPENDIX A
MATHCAD CODE FOR MASS-SPRING ANALYSIS

ORIGIN≡0

$k := 5 \cdot 10^{6} \left(\frac{N}{mm}\right)$ $M := 0.5$ (t) $\omega := \sqrt{\frac{k}{M}} = 3.162 \times 10^{3} \left(\frac{rad}{sec}\right)$

$\alpha := 10 \cdot 10^{10} \left(\frac{N}{sec}\right)$ $\alpha 2 := 20 \cdot 10^{10} \left(\frac{N}{sec}\right)$

$Xcr := 1$ (mm)

stage 1: forcing vibration, v0=u0=0

$t := 0.0000000$

Given

$Xcr = \frac{\alpha}{k} \cdot \left(t - \frac{\sin(\omega \cdot t)}{\omega}\right)$

$tf := Find(t)$ $tf = 3.159 \times 10^{-4}$

$t := 0.0000000$

Given

$Xcr = \frac{\alpha 2}{k} \cdot \left(t - \frac{\sin(\omega \cdot t)}{\omega}\right)$

$tf2 := Find(t)$ $tf2 = 2.492 \times 10^{-4}$

$P(\alpha, t) := \alpha \cdot t$ $x(\alpha, t) := \frac{\alpha}{k} \cdot \left(t - \frac{\sin(\omega \cdot t)}{\omega}\right)$ $ma(\alpha, t) := \frac{\alpha \cdot \sin(\omega \cdot t)}{\omega}$ $Fs(\alpha, t) := P(\alpha, t) - ma(\alpha, t)$

$FsK := k \cdot Xcr$ $FsK = 5 \times 10^{6}$ (N)

$Fs(\alpha, tf) = 5 \times 10^{6}$ (N) $Fs(\alpha 2, tf2) = 5 \times 10^{6}$ (N)

$P(\alpha, tf) = 3.159 \times 10^{7}$ (N) $P(\alpha 2, tf2) = 4.984 \times 10^{7}$ (N)

stage 2:

free vibration, u0 and v0 are not zero

$$u0(\alpha,\tau) := \frac{\alpha}{k}\cdot\left(\tau - \frac{\sin(\omega\cdot\tau)}{\omega}\right) \qquad v0(\alpha,\tau) := \frac{\alpha}{k}\cdot(1-\cos(\omega\cdot\tau))$$

$$Es(\alpha,\tau) := 0.5k\cdot u0(\alpha,\tau)^2 \qquad Ek(\alpha,\tau) := 0.5M\cdot v0(\alpha,\tau)^2$$

$$We(\alpha,\tau) := Es(\alpha,\tau) + Ek(\alpha,\tau)$$

$$xf(\alpha,\tau) := \sqrt{\frac{2\cdot We(\alpha,\tau)}{k}}$$

$\tau := tf \qquad \tau = 3.159\times 10^{-4}$ (s)

$u0(\alpha,\tau) = 1$ (in)

$v0(\alpha,\tau) = 9.179\times 10^{3}$ $\left(\frac{in}{sec}\right)$

$Es(\alpha,\tau) = 2.5\times 10^{6}$ (N·mm)

$Ek(\alpha,\tau) = 2.106\times 10^{7}$ (N·mm)

$We(\alpha,\tau) = 2.356\times 10^{7}$ (N·mm)

$xf(\alpha,\tau) = 3.07$ (mm)

$\tau 2 := tf2 \qquad \tau 2 = 2.492\times 10^{-4}$ (s)

$u0(\alpha 2,\tau 2) = 1$ (in)

$v0(\alpha 2,\tau 2) = 1.179\times 10^{4}$ $\left(\frac{in}{sec}\right)$

$Es(\alpha 2,\tau 2) = 2.5\times 10^{6}$ (N·mm)

$Ek(\alpha 2,\tau 2) = 3.475\times 10^{7}$ (N·mm)

$We(\alpha 2,\tau 2) = 3.725\times 10^{7}$ (N·mm)

$xf(\alpha 2,\tau 2) = 3.86$ (mm)

$$Ecr := 0.5k\cdot Xcr^2 \qquad Ecr = 2.5\times 10^{6} \quad (N\cdot mm)$$

$$exE(\alpha,\tau) := We(\alpha,\tau) - Ecr$$

$exE(\alpha,\tau) = 2.106\times 10^{7}$ (N·mm)

$exE(\alpha 2,\tau 2) = 3.475\times 10^{7}$ (N·mm)

$$x2(\alpha, t, \tau) := \begin{array}{l} \text{if } t < \tau \\ \quad \text{"forced vibration"} \\ \quad u \leftarrow \frac{\alpha}{k} \cdot \left(t - \frac{\sin(\omega \cdot t)}{\omega} \right) \\ \text{otherwise} \\ \quad \text{"free vibration"} \\ \quad u \leftarrow u0(\alpha, \tau) \cdot \cos[\omega \cdot (t - \tau)] + \frac{v0(\alpha, \tau)}{\omega} \cdot \sin[\omega \cdot (t - \tau)] \\ \text{return } u \end{array}$$

APPENDIX B
MATHCAD CODE FOR P-I CURVE

contstant load

ORIGIN≡ 0

Example data:

$W := 500($ (p) $\quad g := 386.1\left(\frac{in}{sec^2}\right) \quad m := \frac{W}{g} = 12.95 \left(\frac{p \cdot sec^2}{in}\right) \quad k := 1000($ $\left(\frac{p}{in}\right)$

$\omega := \sqrt{\frac{k}{m}} = 27.788 \left(\frac{rad}{sec}\right) \quad T := \frac{2 \cdot \pi}{\omega} = 0.226$ (sec) $\quad Xcr := 0.2$ (in)

$Ecr := 0.5k \cdot Xcr^2$

PI curve

Guess:

$t := 0.0000$

Given

$X = \frac{F}{k} \cdot (1 - \cos(\omega \cdot t))$

$convertXintoT(k, \omega, X, F) := Find(t)$

$i := 0..100$

$Pasm := 0.5k \cdot Xcr = 1 \times 10^3$

$P_i := Pasm + 100 \cdot i \qquad Xwork_i := \frac{Ecr}{P_i}$

$tfWork_i := convertXintoT\left(k, \omega, Xwork_i, P_i\right)$

$Pn_i := \frac{P_i}{k \cdot Xcr}$

$Iallowed := \sqrt{m \cdot k} \cdot Xcr = 71.972$

$Ispecific_i := P_i \cdot tfWork_i$

$$InSpecific_i := \frac{Ispecific_i}{\sqrt{m \cdot k} \cdot Xcr}$$

LIST OF REFERENCES

Bazant, Z., & Kazemi, M. (1991). Size effect on diagonal shear failure of beams without stirrups. *ACI Structural Journal , 88* (3), 268-276.

Baznat, Z. P., & Planas, J. (1998). *Fracture and size effect in concrete and other quasibrittle materials.* CRC Press.

Bischoff, P. H., & Perry, S. H. (1991). Compression behaivior of concrete at high strain rates. *Materials and Structures , 24* (6), 425-450.

CEB. (1993). CEB-FIB model code 1990. Thomas Telford.

Chandra, D., & Krauthammer, T. (1995). Strength enhancement in particular solids under high loading rates. *Earthquake Engineering & Structural Dynamics , 24*, 1609-1622.

Hillerberg, A., Modeer, M., & Peterson, P. E. (1976). Analysis of crack formation and crack growth in concrete by means of fracture mechanics and finite elements. *Cement and Concrete Research, Vol. 6 , 6* (6), 773-781.

Hsu, T. (1993). *Unified theory of reinforced concrete.* CRC Press.

Inglis, C. E. (1913). Stresses in a plate due to the presence of cracks and sharp corners. *Proc.Inst.Naval Archit , 60*, 219-230.

Kolsky, H. (1949). An Investigation of the Mechanical Properties of Materials at Very High Rates of Loading. *Proceedings of the Physical Society , 62*, 676.

Krauthammer, T. (2008). Modern protective structures. CRC Press.

Krauthammer, T., & Elfahal, M. M. (2002). *Size effect in normal and high-strength concrete cylinders subjected to static and dynamic axial compressive loads.* The Pennsylvania state University.

Lessard, M., Challal, O., & Aiticin, P. C. (1993). Testing high strength concrete compressive strength. *ACI Materials Journal , 90* (4).

Park, J. Y., & Krauthammer, T. (2006). *Fracture-based size and rate effects of concrete members.* The Pennsylvania state University.

Ross, C., Kuennen, S., & Strickland, W. (1989). High strain rate effects on tensile strength of concrete. *Fourth international symposium on the interaction of non-nuclear munitions with structures*, *1*, pp. 302-308.

Rossi, P. (1991). Influence of cracking in presence of free water on the mechanical behavior of concrete. *Magazine of concrete research , 43* (154), 53-57.

Shah, S. P., Swartz, S. E., & Ouyang, C. (1995). *Fracture Mechanics of Concrete.* Wiley-Interscience.

Simulia. (2010). *Abaqus version 6.10 documentation.* Dassault Systèmes Simulia Corp.

Timoshenko, S. (1937). Vibration problems in Engineering. D. Van Nostrand Company.

Timoshenko, S., & Goodier, J. N. (1951). Theory of elasticity. McGraw-Hill Book Company.

Weerheijm, J. (1992). *Concrete under impact tensile loading and lateral compression.*

Zhang, X. X., Ruiz, G., & Yu, R. C. (2008). Experimental study of combined size and strain rate effects on the fracture of reinforced concrete. *Journal of Materials in Civil Engineering , 20*, 544.

Zhou, X. Q., & Hao, H. (2008). Mesoscale modelling of concrete tensile failure mechanism at high strain rates. *Computers & Structures , 86* (21-22), 2013-2026.

BIOGRAPHICAL SKETCH

Liran Hadad was born in Israel in 1981. He attended secondary school and junior college in Israel. He was drafted into the army for his national service from 2000 to 2004. He began his undergraduate studies at Ben-Gurion University, Israel, in October 2004 and obtained his Bachelor of Engineering degree in civil engineering on July 2008. In August 2008, he joined Bateman Litwin LTD, Israel, as a structural engineer. In 2009, he began his master's degree in civil engineering at the University of Florida, specializing in protective structures.